Greedy Heuristics for Sampling-based Motion Planning in High-Dimensional State Spaces

Phone Thiha Kyaw, Anh Vu Le, Lim Yi, Prabakaran Veerajagadheswar, Minh Bui Vu and Mohan Rajesh Elara

arXiv:2405.03411v2 [cs.RO] 27 Oct 2024

***Abstract*—Informed sampling techniques improve the convergence rate of sampling-based planners by guiding the sampling toward the most promising regions of the problem domain, where states that can improve the current solution are more likely to be found. However, while this approach significantly reduces the planner's exploration space, the sampling subset may still be too large if the current solution contains redundant states with many twists and turns. This article addresses this problem by introducing a greedy version of the informed set that shrinks only based on the maximum heuristic cost of the state along the current solution path. Additionally, we present Greedy RRT* (G-RRT*), a bi-directional version of the anytime Rapidly-exploring Random Trees algorithm that uses this greedy informed set to focus sampling on the promising regions of the problem domain based on heuristics. Experimental results on simulated planning problems, manipulation problems on Barrett WAM Arms, and on a self-reconfigurable robot, Panthera, show that G-RRT* produces asymptotically optimal solution paths and outperforms state-of-the-art RRT* variants, especially in high dimensions.**

***Index Terms*—Sampling-based path planning, Optimal path planning, Informed sampling, Bidirectional search, Greedy heuristics, High-dimensional planning, Reconfigurable robotic.**

I. Introduction

ROBOT path planning determines a collision-free geometric path from an initial state to a goal state while considering some specific optimizing objectives such as energy or distance travelled [1]. It is a fundamental research area in robotics, and many efforts have been made to develop a wide variety of path planning techniques, including graph-based searches, artificial potential fields, and sampling-based methods [2]. Unfortunately, it is challenging to find collision-free and optimal paths, especially in continuous search spaces or in high dimensions, and this task is generally known to be a PSPACE-hard computational problem [3].

This research is supported by the National Robotics Programme under its National Robotics Programme (NRP) BAU, Ermine III: Deployable Reconfigurable Robots, Award No. M22NBK0054 and also, it is supported by the National Robotics Programme under its National Robotics Programme (NRP) BAU, PANTHERA 2.0: Deployable Autonomous Pavement Sweeping Robot through Public Trials, Award No. M23NBK0065.

(Corresponding author: Anh Vu Le.)

Phone Thiha Kyaw, Lim Yi, Prabakaran Veerajagadheswar and Mohan Rajesh Elara are with the ROAR Lab, Engineering Product Development, Singapore University of Technology and Design, Singapore 487372, Singapore (e-mail: mlsdphonethk@gmail.com; yi_lim@mymail.sutd.edu.sg; prabakaran@sutd.edu.sg; rajeshelara@sutd.edu.sg).

Anh Vu Le is with Optoelectronics Research Group, Faculty of Electrical and Electronics Engineering, Ton Duc Thang University, Ho Chi Minh City 700000, Vietnam (e-mail: leanhvu@tdtu.edu.vn).

Minh Bui Vu is with Faculty of Engineering and Technology, Nguyen Tat Thanh University, 300A - Nguyen Tat Thanh, Ward 13, District 4, Ho Chi Minh City, Vietnam (e-mail: bvminh@ntt.edu.vn).

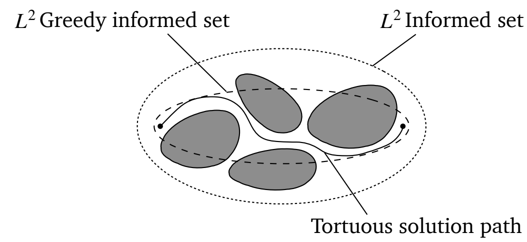

Fig. 1: Comparison between relative sizes of the informed sets in planning problems with tortuous solution paths. The L^2 informed set is estimated based on the current solution cost, therefore having the larger ellipsoidal area. The L^2 greedy informed set, on the other hand, only uses the heuristic cost of the state in the current solution with maximum admissible heuristics, thereby reducing the size of the hyperellipsoid.

In order to achieve computational efficiency in high-dimensional continuous state spaces, sampling-based planning algorithms have been proposed, such as probabilistic roadmaps (PRM) [4] and Rapidly-Exploring Random Trees (RRT) [5]. Compared to traditional complete graph-search approaches such as Dijkstra's algorithm [6] or A* [7], these sampling-based algorithms relax the completeness requirements and find feasible solutions faster in continuous state spaces with *probabilistic completeness* guarantees, i.e., the probability that the algorithm fails to find the solution, if one exists, decays to zero as the number of samples approaches infinity. Additionally, extensions have been developed to propose *anytime* favor sampling-based approaches such as PRM* and RRT* [8], which not only hold probabilistic completeness guarantees and also have *asymptotic optimality* property, i.e., the algorithm almost-surely converges towards the optimum as the number of samples approaches infinity.

These anytime sampling-based algorithms are very effective in finding optimal solutions to high-dimensional continuous path planning problems. Like RRTs, these approaches rely on random sampling to explore the search space of the problem domain (i.e., incrementally expanding the tree through free space). Unlike RRTs, they extend this process by locally optimizing every added vertex (i.e., incrementally rewiring the tree during the expansion process). This rewiring ensures that RRT* asymptotically converges to the optimal solution if given enough time. However, it is inefficient to rely on a random sampling approach, especially in large problem domains or high-dimensional state spaces, as a significant amount of computational effort can be wasted on states that do not contribute to improving the current solution or on

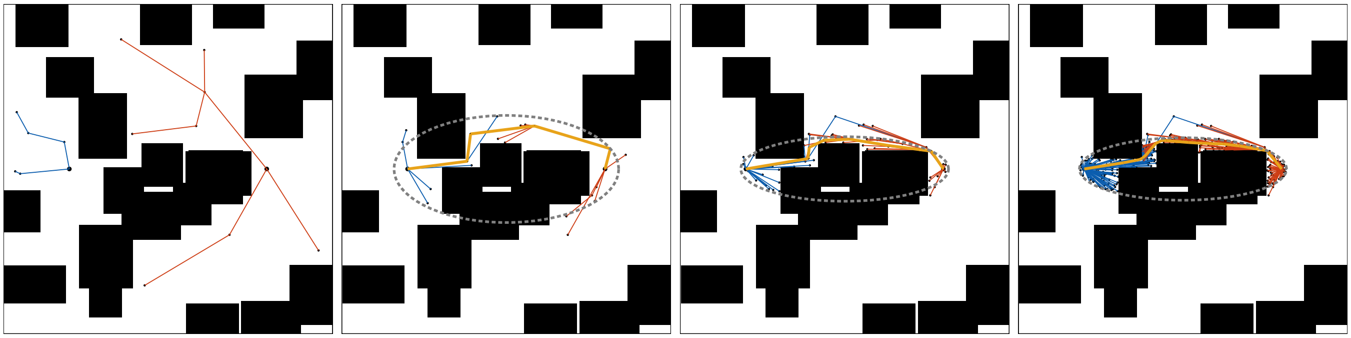

(a) (b) (c) (d)

Fig. 2: Illustrations of the progress of sampling-based bi-directional search performed by the G-RRT* algorithm. The initial and goal states are represented by big black dots, whereas the sampled states are represented by small black dots. The start and goal trees constructed to explore the state space are shown in blue and orange, respectively, while the current solution is highlighted in yellow. The set of states that could produce better solution costs than the heuristic cost of the greedily chosen state in the current solution (the L^2 greedy informed set) is highlighted with gray dashed lines. G-RRT* starts the exploration of the problem domain by maintaining two rapidly growing trees, one rooted in the initial state and one in the goal state (a). The expansion of the search of these two trees is guided by a greedy connection heuristic, leading towards each other to form an initial solution (b). The search then only focuses on the states that are inside the greedy informed set defined by the current solution path, improving the accuracy with more focused sampled states (c). G-RRT* repeats these steps within the available time budget and almost-surely asymptotically converges towards the optimal solution (d).

exploring unnecessary regions of the planning domain.

Therefore, researchers have investigated several techniques to develop extended versions of RRT and RRT*-based algorithms. Ferguson and Stentz [9] proposed an anytime version of RRT by reusing information from previous trees to improve the quality of the current tree and solution path within the allocated time. They found that limiting nodes with a lower cost bound relative to the previous solution cost can increase the probability of finding better solutions. Such similar sample rejection ideas have been integrated into RRT* to further improve its convergence rate towards the optimum [10, 11]. Building on these concepts, Gammell et al. [12] introduced the direct informed sampling technique in their Informed RRT* algorithm, which exploits the current solution path to focus the search on promising regions of the planning domain, thereby improving the convergence rate of RRT*.

Informed RRT* limits the exploration space of RRT* by directly sampling within a hyperellipsoid determined by the current path cost. This approach significantly outperforms RRT* in terms of convergence rate and final solution quality while maintaining a uniform sample distribution over the informed subset, ensuring optimal guarantees. However, the initial solution paths found by the planner may be tortuous, containing a large number of redundant states. As a result, this leads to unnecessarily larger informed sets, which slow down the exploration and convergence process, especially in high-dimensional spaces.

This article addresses the computational burden associated with the informed hyperellipsoid proposed in Informed RRT* by introducing a new direct informed sampling procedure. Our approach biases sampling based on heuristic information from the states in the current solution path, regardless of their cost, thereby mitigating the impact of tortuous initial solution paths. Specifically, we propose a *greedy informed set*, a subset of the informed set that greedily exploits information from the current solution path to rapidly reduce the size of the informed exploration hyperellipsoid, enhancing sampling efficiency (Figure 1).

Applying direct informed sampling techniques to RRT* does indeed improve the convergence rate of the algorithm, as the search is focused within hyperellipsoids. However, in certain planning scenarios where the initial path takes longer to find, the advantages of a focused search become impractical. One way to find faster initial solutions is to use a bidirectional approach. Bidirectional versions of RRT, such as RRT-Connect [13], grow two trees—one rooted at the start and one at the goal—to explore the problem state space and use a greedy connection heuristic to guide the trees towards each other. Therefore, this article improves the efficiency of initial solution times in planners that use focused sampling techniques by incorporating bidirectional search concepts.

Expanding on these greedy heuristics, this paper presents Greedy RRT* (G-RRT*), an almost surely asymptotically optimal sampling-based planning algorithm utilizing bidirectional search. G-RRT* is introduced to demonstrate the benefits of employing greedy search and heuristic techniques in sampling-based planning to achieve practical performance in high-dimensional state spaces. It highlights the importance of exploiting the search space to improve sample efficiency through the use of a greedy informed set. Additionally, it shows the necessity of maintaining dual rapidly exploring trees in high-dimensional planning to avoid local minima and to quickly find initial solutions (Figure 2).

The benefits of exploiting the problem state space with greedy heuristics are demonstrated through simulated planning problems in $\mathbb{R}^2$, $\mathbb{R}^4$, $\mathbb{R}^8$, and $\mathbb{R}^{16}$; manipulation problems on Barrett WAM arms in $\mathbb{R}^{14}$; and on a robotic platform, Panthera—a 5-degree-of-freedom self-reconfigurable mobile robot [14] (Section VI). All planning problems are tested with the objective of minimizing path length. These experiments show that our approach is capable of finding quick initial solutions with a faster convergence rate and outperforms state-of-the-art methods, particularly in scenarios involving large planning domains.

This article is organized as follows. Section II describes the path planning problem definition and provides an overview of sampling-based path planning, as well as background on accelerating RRT* convergence through sampling. Section III defines the greedy informed set, which is demonstrated with the G-RRT* algorithm in Section IV. Section V analyzes the theoretical guarantees of G-RRT*. Section VI examines and demonstrates G-RRT* in simulations and in real-world experiments with a self-reconfigurable robot, Panthera. Finally, the article concludes with a discussion and future research plans in Section VII.

A. Statement of Contributions

This article is a continuation of the ideas of the greedy informed set first introduced in our previous work [15], with a focus on formal guarantees, where we analyze the optimality of the greedy informed set, and demonstrates a novel informed sampling-based planning algorithm through extensive experimental evaluations. Specifically, it makes the following contributions:

- Provides a formal analysis of the greedy informed set, focusing on how exploitation with heuristics affects optimality (Section III, Theorems 1 and 2)
- Presents Greedy RRT* (G-RRT*), a bi-directional asymptotically optimal sampling-based planning algorithm, as an extension of RRT* that leverages the greedy heuristic concepts (Section IV).
- Proves the completeness and asymptotic optimality of G-RRT* by building upon findings from the sampling-based planning literature (Section V, Theorem 3).
- Demonstrates experimentally that the benefits of greedy exploitation in large planning domains yield better success and convergence rates than state-of-the-art algorithms, through simulations and on a real-world robotic platform (Section VI).

II. Preliminaries and Background

This section first presents a formal definition of the optimal path planning problem (Section II-A) and then reviews the existing literature on sampling-based planning algorithms (Section II-B) and methods for accelerating the convergence of these asymptotically optimal planners based on the distribution of samples in the state space (Section II-C).

A. Problem Formulation

In robotics, the path planning problem is commonly distinguished into two problems, namely: *feasible* and *optimal* planning [8]. Feasible path planning finds a collision-free path from an initial location to a target location. Therefore, there are many possible solutions in feasible planning problems. Optimal path planning, on the other hand, finds the best unique feasible path based on the given optimization objective. The following definitions given in Definition 1 and 2 formally describe the feasible and optimal path planning problems.

Definition 1 (The feasible path planning problem)**.** *Let $\mathcal{X} \in \mathbb{R}^n$ be the state space of the geometric planning problem. Let $\mathcal{X}_{obs} \subseteq \mathcal{X}$ be the set of all states, $\mathbf{x}$, that are in collision with obstacles, $\mathcal{O}$, and $\mathcal{X}_{free} = \mathcal{X} \setminus \mathcal{X}_{obs}$ be the resultant collision-free set. Let $\mathbf{x}_I \in \mathcal{X}_{free}$ be the initial state and $\mathbf{x}_G \in \mathcal{X}_{free}$ be the goal state. Let $\pi : [0,1] \to \mathcal{X}_{free}$ be a feasible path in continuous domain and Σ be the set of all non-trivial solution paths. The feasible path planning problem is then formally defined as to find any path $\pi' \in \Sigma$ in (1) from this set that connects $\mathbf{x}_I$ to $\mathbf{x}_G$ through collision-free space,*

$$\pi' \in \Big\{\pi \in \Sigma \mid \pi(0) = \mathbf{x}_I,\ \pi(1) = \mathbf{x}_G, \\ \forall s \in [0,1],\ \pi(s) \in \mathcal{X}_{free}\Big\}. \tag{1}$$

Definition 2 (The optimal path planning problem)**.** *The optimal path planning problem is formally defined as to find a feasible path π^* in (2) from $\mathbf{x}_I$ to $\mathbf{x}_G$ through collision-free space that minimizes the given cost objective, $c : \Sigma \to \mathbb{R}_{\geq 0}$,*

$$\pi^* = \arg\min_{\pi \in \Sigma}\Big\{c(\pi) \mid \pi(0) = \mathbf{x}_I,\ \pi(1) = \mathbf{x}_G, \\ \forall s \in [0,1],\ \pi(s) \in \mathcal{X}_{free}\Big\}, \tag{2}$$

where Σ denotes the set of all non-trivial paths and $\mathbb{R}_{\geq 0}$ is the set of non-negative real numbers.

Formal guarantees provided by sampling-based algorithms concerning these feasible or optimal planning problems are often probabilistic in nature. An algorithm is considered to be *probabilistically complete* (Definition 3) when, given an infinite number of samples, the probability of finding a solution, should one exist, approaches one. Furthermore, an algorithm is described as *almost-surely asymptotically optimal* (Definition 4) if, with an increasing number of samples, it converges asymptotically to the optimal solution with a probability of one, provided that an optimal solution exists [8]. Note that almost-sure asymptotic optimality implies probabilistic completeness.

Definition 3 (Probabilistic completeness)**.** *A sampling-based path planning algorithm is said to be probabilistically complete if, as the number of samples approaches infinity, the probability of finding a feasible solution (Definition 1) converges to one,*

$$\liminf_{n\to\infty} \mathbb{P}(\pi_n \in \Sigma, \pi_n(0) = \mathbf{x}_I, \pi_n(1) = \mathbf{x}_G) = 1, \tag{3}$$

where n is the number of samples and π_n is the path from the initial state to the goal state found by the algorithm from those samples.

Definition 4 (Almost sure asymptotic optimality)**.** *A sampling-based path planning algorithm is said to be almost-surely asymptotic optimal if, as the number of samples approaches* *infinity, the probability of asymptotically converging to the optimum (Definition 2), if an optimal solution exists, is one,*

$$\mathbb{P}\Big(\limsup_{n\to\infty}\min_{\pi\in\Sigma_n}\{c(\pi)\}=c^*\Big)=1, \tag{4}$$

where n is the number of samples, $\Sigma_n\subset\Sigma$ is the set of all non-trivial paths found by the algorithm from those samples and c^* is the optimal solution cost.

B. Sampling-based motion planning

Sampling-based planning algorithms can be classified into multiple-query and single-query categories. Multiple-query planners construct a graph (roadmap) representing collision-free paths that can be queried with multiple initial and goal states by computing the shortest path from the initial state to the goal state. In contrast, single-query planners only focus on individual initial and goal state pairs. The most commonly used algorithms for multiple-query applications are probabilistic roadmaps (PRMs) [4, 16], while rapidly-exploring random trees (RRTs) [5] are typically used for single-query applications. These sampling-based planners are often effective in high-dimensional state spaces and save a significant amount of computation by avoiding an explicit representation of obstacles in the state space, as opposed to deterministic methods such as graph search-based planners. However, these planners only generate feasible solutions (collision-free paths), which may not be guaranteed to be optimal.

Karaman and Frazzoli [8] propose new sampling-based multiple and single-query planners, PRM* and RRT*, the variants of PRMs and RRTs that provide optimality guarantees. RRT* works in a similar way to RRT by incrementally expanding a tree into the free space, guided by randomly sampled states. However, unlike RRT, it takes into account nearby vertices surrounding the randomly sampled state to ensure that the most suitable parent vertex in the tree is selected. Moreover, RRT* also considers the possibility of rewiring nearby vertices in relation to this randomly sampled state. This incremental rewiring process plays a crucial role in guiding RRT* toward asymptotic convergence to the optimal solution, a characteristic of paramount importance in sampling-based motion planning research.

The RRT$^{\#}$ algorithm [17] extends the exploitation process (local rewiring) of RRT* to global rewiring by utilizing dynamic programming methods, resulting in an improvement of the speed of convergence rate. Removal of states that could not improve the current solution will help reduce the time required for convergence. Karaman et al. [18] extend the RRT* by introducing the online graph pruning algorithm called branch-and-bound. Here, a vertex in the current tree is deleted if the cost to reach this vertex plus the lower bound on the optimal cost to reach the goal (similar to the A* admissible heuristic) is more than the cost of the current solution path. These are the vertices that could not improve the current solution, and pruning them does help improve the RRT* convergence time to enable efficient real-time operation. Moreover, modifications have been made to parent selection and rewiring processes of RRT*. Instead of only considering a set of nearby vertices in a hypersphere as in RRT*, Quick-RRT* [19] also considers their ancestry up to a user-defined parameter for possible parent candidates. A similar tree-extending algorithm is introduced in F-RRT* [20], which creates random parent vertices near obstacles to find better initial solutions with a faster convergence rate.

Furthermore, various extensions have been proposed to accelerate the convergence rate, such as bi-directional versions like RRT-Connect [13] and RRT*-Connect [21], as well as methods that relax optimality to near-optimality, including SPARS [22] and LBT-RRT [23]. Nevertheless, since the sampling process of these approaches employs a uniform random distribution over the entire state space, the algorithm's convergence rate decreases as the number of dimensions increases, requiring longer computation times to generate optimal solutions.

C. State-space sampling

Prior work has focused on increasing the efficiency of the random sampling process in sampling-based planning algorithms. Generally, the performance of the planner depends significantly on the distribution of random samples generated in each iteration. Many approaches rely on uniformly distributed samples across the entire state space to ensure that global optimality is preserved. However, performance can often be improved by focusing the sampling on regions with a higher likelihood of finding better solutions.

Bialkowski et al. [24] propose a biased-sampling technique that generates random samples from the approximated obstacle-free distribution space. They demonstrate that the distribution converges to a uniform distribution over the free space as the number of samples approaches infinity. Similarly, Kim et al. [25] decompose the collision-free space into a set of spheres with varying radii, called a sampling cloud. Their Cloud RRT* algorithm exploits this sampling cloud to generate random samples and continuously updates it to refine the current best solution. In the P-RRT* and PQ-RRT* algorithms [26, 27], random samples are directionally guided by artificial potential fields [28] to efficiently explore the given environment. Unlike the traditional rejection sampling approach (i.e., repeatedly sampling from the entire state space until a collision-free sample is found), these free-space biased sampling heuristic techniques quickly find better solutions and reduce the number of rejected samples; however, they continue to sample states that do not improve the current solution.

Prior work has focused on improving the random sampling process and the convergence rate of RRT*. Akgun and Stilman [10] propose a bi-directional version of RRT* that uses path-biased sampling and heuristic sample rejection techniques to accelerate the planner's convergence rate in high-dimensional planning problems. Similarly, these path biasing and path refinement ideas have been employed in [29, 30] to improve the performance of the original RRT*. However, these methods tend to favor finding locally optimal solutions, which decreases the likelihood of obtaining samples that can improve the current solution. Moreover, techniques such as rectangular rejection sampling [9, 11] have also been applied to RRT* to further improve the convergence rate and reduce computational requirements. However, these approaches do not increase the probability of finding better solutions, and their effectiveness decreases as the number of state dimensions grows.

To address these issues and accelerate the convergence of RRT*, a direct informed sampling technique is introduced in [12, 31], which is demonstrated with the Informed RRT* algorithm. Informed RRT* behaves the same as RRT* until an initial solution is found. Once the initial solution is found, it biases the sampling on the subset of the state space (the L^2 informed set), which is an n-dimensional hyperellipsoid with a transverse diameter of the current solution cost. Unlike the aforementioned techniques, this approach maintains the uniform sample distribution over the informed subset and considers all the states that could provide better solutions and is still effective in higher-dimensional state spaces. However, the solution path found by the planner may contain redundant states, leading to tortuous paths with many twists and turns, especially in the early phases of the planning process. This can, in fact, result in an unnecessary path cost with large informed sets, thereby slowing down the convergence rate of the planner. Therefore, recent work has shown great interest in integrating more advanced path refinement techniques with informed sampling to further reduce the size of the hyperellipsoid, thereby accelerating convergence [32, 33, 34]. Nevertheless, these advanced approaches can still be improved by incorporating a greedy informed sampling heuristic (Section III) to facilitate the exploitation process of the sampling-based planning algorithms.

Research has also shown interest in integrating bio-inspired methods [35, 36] and learning sampling heuristics [37, 38, 39] to effectively guide tree growth toward the goal by restricting the sampling state space of the problem domain, achieving a non-uniform sampling distribution.

III. Greedy Informed Set

Informed RRT* has been proposed to improve the convergence rate of the RRT* algorithm by utilizing direct informed sampling techniques, which perform sampling on the ellipsoidal subset of the planning domain, the *L^2 informed set* (Definition 6). This informed subset is an estimate of the *omniscient set* (Definition 5), the set of states that can provide a better solution, and both sets provide the theoretical upper bounds on the probability of improving a solution in problems seeking to minimize path length in $\mathbb{R}^n$—see [31] for more details. However, since the informed set is an admissible estimate of the omniscient set and is approximated based on the current path cost, not all randomly sampled states within the informed subset may lead to an improvement of the current solution path. In other words, this may result in a larger ellipsoidal informed set with redundant samples, taking unnecessary computation time to converge to the optimal solution, especially in higher-dimensional state spaces. For instance, in planning problems with a large number of obstacles and tight spaces, the initial solution paths produced by the algorithm can be tortuous, with many twists and turns, resulting in a substantial informed set with a higher solution cost. Therefore, to improve the algorithm's convergence rate and reduce the size of the subset in these constrained scenarios with tortuous solution paths, this paper proposes a new direct informed sampling strategy that does not rely on the cost of the current solution path. Instead, it uses only the maximum heuristic cost from the existing solution, which can be obtained by finding the heuristic value of the greedily chosen state in the current solution path. This new informed subset accepts only randomly sampled states that can guarantee better solution costs than the heuristic value of the greedily chosen state (Definition 7).

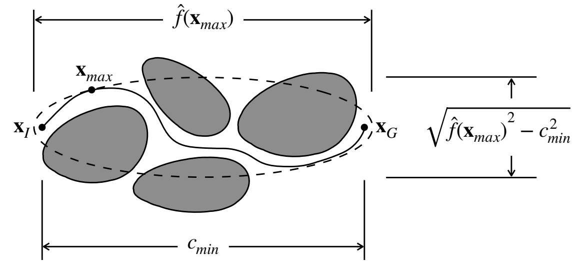

Fig. 3: Illustration of the L^2 greedy informed set, $\mathcal{X}_{\hat{f}_{\text{greedy}}}$, for an $\mathbb{R}^2$ planning problem with path minimizing objectives. This greedy subset is highlighted in an ellipse with a dashed line and determined by the hypothetical minimum cost, c_{min}, from an initial state, $\mathbf{x}_I$, to the goal state, $\mathbf{x}_G$, and the heuristics cost of a state in the solution path with highest admissible estimates, $\hat{f}(\mathbf{x}_{\text{max}})$, as a transverse diameter.

Once an initial solution is found by the planning algorithm, the set of states that can provide a better solution is formally defined as the *omniscient set* (Definition 5).

Definition 5 (Omniscient set)**.** *Let $g(\mathbf{x})$ be the cost-to-come of a state, $\mathbf{x} \in \mathcal{X}$, which represents the true cost of the optimal path from the initial state $\mathbf{x}_I$ to a state $\mathbf{x}$, and let $h(\mathbf{x})$ be the cost-to-go of a state $\mathbf{x}$, which represents the true cost of the optimal path from a state $\mathbf{x}$ to the goal state $\mathbf{x}_G$,*

$$\begin{aligned} g(\mathbf{x}) &= \min_{\pi \in \Sigma} \left\{ c(\pi) \mid \pi(0) = \mathbf{x}_I,\ \pi(1) = \mathbf{x} \right\}, \\ h(\mathbf{x}) &= \min_{\pi \in \Sigma} \left\{ c(\pi) \mid \pi(0) = \mathbf{x},\ \pi(1) = \mathbf{x}_G \right\}. \end{aligned} \tag{5}$$

Let $f(\mathbf{x})$ be the true cost of the optimal path from the initial state $\mathbf{x}_I$ to the goal state $\mathbf{x}_G$, constrained to pass through $\mathbf{x}$, i.e., $f(\mathbf{x}) = g(\mathbf{x}) + h(\mathbf{x})$. We then define the omniscient set*, $\mathcal{X}_f$, as the set of states in collision-free space, $\mathcal{X}_{free}$, that can provide better solutions than the current solution cost, c_i,*

$$\mathcal{X}_f = \left\{ \mathbf{x} \in \mathcal{X}_{free} \mid f(\mathbf{x}) < c_i \right\}. \tag{6}$$

Although sampling from this omniscient set is a necessary condition for RRT*-like planners to improve the current solution, the exact knowledge of the set is unknown and requires solving the planning problem. Therefore, the estimates of the set are required to provide better solutions while maintaining the theoretical upper bounds (Definition 6).

Definition 6 (L^2 Informed set)**.** *Let the functions $\hat{g}(\mathbf{x})$ and $\hat{h}(\mathbf{x})$ be the L^2 heuristic values of the cost-to-come of a state,*

$\mathbf{x} \in \mathcal{X}$*, from the initial state,* $\mathbf{x}_I$*, and the cost-to-go from a state to the goal state,* $\mathbf{x}_G$*, respectively,*

$$\begin{aligned}\hat{g}(\mathbf{x}) &= \|\mathbf{x} - \mathbf{x}_I\|_2 \\ \hat{h}(\mathbf{x}) &= \|\mathbf{x}_G - \mathbf{x}\|_2\end{aligned} \tag{7}$$

where $\|.\|_2$ *denotes the* L^2 *norm (i.e., Euclidean distance) between two states. Let the function* $\hat{f}(\mathbf{x})$ *be the* L^2 *heuristic cost of a solution path from* $\mathbf{x}_I$ *to* $\mathbf{x}_G$ *constrained to pass through* $\mathbf{x}$*, i.e.,* $\hat{f}(\mathbf{x}) = \hat{g}(\mathbf{x}) + \hat{h}(\mathbf{x})$*. We then define the* L^2 informed set*,* $\mathcal{X}_{\hat{f}}$*, as the set of states whose heuristic estimates can provide better solutions than the current solution cost,* c_i*,*

$$\mathcal{X}_{\hat{f}} = \left\{ \mathbf{x} \in \mathcal{X}_{\mathit{free}} \mid \hat{f}(\mathbf{x}) < c_i \right\}. \tag{8}$$

Moreover, this set provides an upper bound estimate of the omniscient set and contains all the states that can yield better solutions, i.e., $\mathcal{X}_{\hat{f}} \supseteq \mathcal{X}_f$, if its heuristic estimates never overestimate the path's true cost (*admissible heuristics*),

$$\forall \mathbf{x} \in \mathcal{X}, \ \hat{f}(\mathbf{x}) \leq f(\mathbf{x}). \tag{9}$$

Therefore, sampling or adding states from an admissible informed set is a necessary condition for improving the current solution and maintaining the uniform sample distribution to ensure asymptotic optimality guarantees [31].

However, in the case of complex planning problems with many homotopy classes, the initial solution paths found by the planner may contain several twists and turns, resulting in larger informed sets. This can, in fact, slow down the convergence rate of the planner, especially in high-dimensional state spaces, since the heuristic does not provide substantial information. In other words, there is a very low chance of drawing a random sample from the informed set that could also belong to the omniscient set. Hence, instead of relying on the existing solution cost to construct these large informed sets, the states that found the existing solution path can be utilized to build a decreasing series of ellipses that are bounded from above by the admissible informed sets (Definition 7).

Definition 7 (L^2 Greedy informed set)**.** *Let* $\mathbf{x}_{\mathit{max}}$ *be the state in the current solution path,* π_i*, with the maximum admissible heuristic cost,*

$$\mathbf{x}_{\mathit{max}} := \underset{\mathbf{x} \in \pi_i}{\arg\max} \left\{ \hat{f}(\mathbf{x}) \right\}. \tag{10}$$

We then define the L^2 greedy informed set*,* $\mathcal{X}_{\hat{f}_{\mathit{greedy}}}$*, as the set of all states in obstacle-free space that could produce better solution costs than the heuristic cost of this greedily chosen state* $\mathbf{x}_{\mathit{max}}$ *in the current solution (Figure 3),*

$$\mathcal{X}_{\hat{f}_{\mathit{greedy}}} = \left\{ \mathbf{x} \in \mathcal{X}_{\mathit{free}} \mid \hat{f}(\mathbf{x}) < \hat{f}(\mathbf{x}_{\mathit{max}}) \right\}. \tag{11}$$

Furthermore, it is bounded from above by the informed set, i.e., $\mathcal{X}_{\hat{f}_{\text{greedy}}} \supseteq \mathcal{X}_{\hat{f}}$ and will lead to smaller ellipsoidal regions compared to the original informed set, particularly in high-dimensional planning scenarios with complex solution paths. Consequently, sampling from this smaller subset will increase the likelihood of finding states that could belong to the omniscient set, thus facilitating faster convergence rates in improving the current solution path. However, because the greedy informed set is constructed based on the exploited knowledge of the existing solution path, similar to path biasing methods, it may or may not contain all the samples from the omniscient set, potentially seeking locally optimal solutions in certain planning contexts. Therefore, exploration into other homotopy classes—i.e., sampling from the informed set—remains essential for planners utilizing the greedy informed set to ensure global optimality and hold asymptotic optimality guarantees (see Section IV).

Sampling informed sets is a necessary condition for ensuring asymptotic optimality in planning problems, as states from the optimal path always lie within these sets [31]. The greedy informed set also includes states from the optimal path, but only under the condition that the current path and the true optimal path lie within the same homotopy class (Theorem 1). This condition offers a reasonable approximation that relaxes some of the optimality constraints of informed sets while still providing faster convergence and optimality guarantees under certain conditions. The motivation behind the proposed greedy heuristic approximation stems from the observation that, for many holonomic planning problems seeking to minimize path length, this relaxation is often sufficient to produce high-quality solutions.

In the following, we will draw on concepts from homotopy theory [40] to formalize the optimality proof of the greedy informed set (Theorem 1) and present a counterexample illustrating cases where it fails to find the optimal solution (Theorem 2). First, we present the formal definition of the path homotopy (Definition 8).

Definition 8 (Homotopy class)**.** *Two paths* π *and* π^* *are said to be path homotopic if they have the same initial and goal states* $\mathbf{x}_I$ *and* $\mathbf{x}_G$ *and if there exists a continuous function* $f : [0,1] \times [0,1] \to \mathcal{X}$ *(called a homotopy) such that:*

- $f(s, 0) = \pi(s)$,
- $f(s, 1) = \pi^*(s)$,
- $f(0, t) = \mathbf{x}_I$,
- $f(1, t) = \mathbf{x}_G$,

for each $s \in [0, 1]$ *and each* $t \in [0, 1]$*. Then the paths* π *and* π^* *are said to be in the same homotopy class.*

The following lemma establishes a connection between the notions of homotopic paths and collision-free space.

Lemma 1 (Homotopic paths can be continuously deformed into each other)**.** *Let* π *and* π^* *be two paths from the initial state,* $\mathbf{x}_I$ *to the goal state,* $\mathbf{x}_G$*, in the same homotopy class. Then, there exists a continuous deformation* $f : [0,1] \times [0,1] \to \mathcal{X}_{\mathit{free}}$ *such that:*

$$f(0, \cdot) = \pi \quad \textit{and} \quad f(1, \cdot) = \pi^*,$$

and for each $t \in [0, 1]$*,* $f(t, \cdot)$ *is a valid collision-free path.*

Proof. By the definition of homotopy (Definition 8), two paths π and π^* in the same homotopy class can be continuously deformed into each other while having the same initial and goal states fixed. This deformation guarantees that for any $t \in [0, 1]$, the path $f(t, \cdot)$ is feasible and stay within the collision-free configuration space $\mathcal{X}_{\text{free}}$. Hence, π and π^* are connected via a continuous deformation in $\mathcal{X}_{\text{free}}$. $\square$

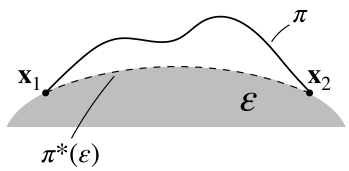

Fig. 4: Illustration of the geodesic path between two states, $\mathbf{x}_1$ and $\mathbf{x}_2$, on an ellipsoid, $\mathcal{E}$, in $\mathbb{R}^2$. The geodesic path, $\pi^*(\mathcal{E})$, is shown with a dashed line, while a higher-cost path, π, which passes outside the ellipsoid, is depicted with a solid line. The ellipsoid $\mathcal{E}$ is partially highlighted in the gray-shaded region.

Next, we want to establish that this property still holds for subpaths of homotopic paths.

Lemma 2 (Subpaths of homotopic paths can also be continuously deformed into each other)**.** *Let π and π^* be two paths from the initial state $\mathbf{x}_I$ to the goal state $\mathbf{x}_G$ that are homotopic in the same homotopy class. If $\pi_{[a,b]}$ is any subpath of π and $\pi^*_{[c,d]}$ is any subpath of π^*, then there exists a continuous deformation that allows $\pi_{[a,b]}$ to be deformed into $\pi^*_{[c,d]}$.*

Proof. Consider the intervals $[a, b]$ and $[c, d]$ corresponding to the subpaths $\pi_{[a,b]}$ and $\pi^*_{[c,d]}$, respectively. The function $g : [0, 1] \times [a, b] \to \mathcal{X}_{\text{free}}$ can be defined as follows:

$$g(t, s) = f(t, s),\ s \in [a, b]$$

At $t = 0$, the deformation begins with:

$$g(0, s) = f(0, s) = \pi(s) \quad \text{for } s \in [a, b],$$

and at $t = 1$, the deformation concludes with:

$$g(1, s) = f(1, s) = \pi^*(s) \quad \text{for } s \in [c, d].$$

Thus, the function $g(t, s)$ represents a continuous transformation that allows $\pi_{[a,b]}$ to be deformed into $\pi^*_{[c,d]}$. Since $f(t, \cdot)$ is a valid collision-free path for every t (Lemma 1), the deformation $g(t, s)$ remains within $\mathcal{X}_{\text{free}}$ throughout the deformation process. Hence, the conclusion is reached that any subpath of π can be continuously deformed into any subpath of π^* as long as both paths are homotopic. □

Next, we define the geodesic path on an ellipsoid (Definition 9), as it is crucial for establishing the optimality of the greedy informed set, and it is illustrated in Figure 4.

Definition 9 (Geodesic path)**.** *Let $\mathcal{E}$ be an ellipsoid in $\mathbb{R}^n$. Let $\partial\mathcal{E}$ be the boundary of $\mathcal{E}$, and let $\mathbf{x}_1$ and $\mathbf{x}_2$ be the two states on $\partial\mathcal{E}$. Define π^* as the path along the boundary of $\mathcal{E}$ from $\mathbf{x}_1$ to $\mathbf{x}_2$, and let π be the path that traverses outside $\mathcal{E}$ between these two points. We define the geodesic path of $\mathcal{E}$ between $\mathbf{x}_1$ and $\mathbf{x}_2$ as the direct path along the boundary of $\mathcal{E}$ that has minimal cost compared to all other paths that pass outside the ellipsoid between the same two endpoints (Figure 4), i.e.,*

$$\pi^*(\mathcal{E}) = \underset{\pi \in \Sigma}{\arg\min} \Big\{ c(\pi) \mid \pi(0) = \mathbf{x}_1,\ \pi(1) = \mathbf{x}_2, \\ \forall s \in [0, 1],\ \pi(s) \in \mathcal{X}_{\mathit{free}} \cap \partial\mathcal{E} \setminus \mathcal{E} \Big\}.$$

We now present the proof that the optimal path lies within the greedy informed set, given that both the optimal path and the current solution path are in the same homotopy class (Theorem 1). First, it demonstrates a case where the optimal solution lies outside the greedy hyperellipsoid and shows that this violates the optimality condition.

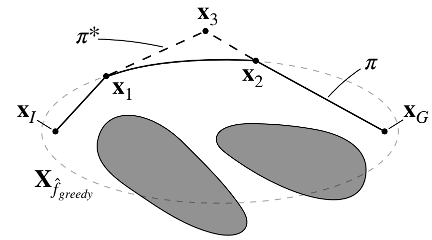

Fig. 5: Illustration of the current solution path π and another path π^* in the same homotopy class, both with the same initial and goal states, $\mathbf{x}_I$ and $\mathbf{x}_G$. The greedy informed set $\mathcal{X}_{\hat{f}_{\text{greedy}}}$ (depicted as a dashed gray ellipse) is constructed based on the maximum heuristic cost along π. The path π^* intersects the boundary of the greedy informed set at states $\mathbf{x}_1$ and $\mathbf{x}_2$, passing through a state $\mathbf{x}_3$, which lies outside $\mathcal{X}_{\hat{f}_{\text{greedy}}}$.

Theorem 1 (Inclusion of the optimal path in the greedy informed set within the same homotopy class)**.** *For a given path π, the greedy informed set $\mathcal{X}_{\hat{f}_{greedy}}(\pi)$ contains the optimal path π^* if π^* is in the same homotopy class as π.*

Proof. Proof of Theorem 1 follows directly from Lemma 2. We begin by constructing an example planning scenario, as depicted in Figure 5, with the details provided below.

Let π be the current solution path in $\mathcal{X}_{\text{free}}$ from the initial state $\mathbf{x}_I$ to the goal state $\mathbf{x}_G$. Denote $\mathbf{x}_1$ and $\mathbf{x}_2$ as two states along the path π that have the same maximum heuristic cost, i.e., $\hat{f}(\mathbf{x}_1) = \hat{f}(\mathbf{x}_2) = \hat{f}(\mathbf{x}_{\text{max}})$. The path π is constructed such that any state $\mathbf{x}$ lying between $\mathbf{x}_1$ and $\mathbf{x}_2$ along the segment of π has the same heuristic cost, i.e.,

$$\forall \mathbf{x} \in \mathcal{Z},\ \hat{f}(\mathbf{x}) = \hat{f}(\mathbf{x}_{\text{max}})$$

where $\mathcal{Z} := \{\mathbf{x} \in \pi' \mid \pi'(0) = \mathbf{x}_1,\ \pi'(1) = \mathbf{x}_2,\ \pi' \subseteq \pi\}$. By Definition 7, the greedy informed set $\mathcal{X}_{\hat{f}_{\text{greedy}}}(\pi)$ is constructed based on $\mathbf{x}_{\text{max}}$ of π. We aim to show that the optimal path π^* also lies inside $\mathcal{X}_{\hat{f}_{\text{greedy}}}$ constructed by π if both π and π^* are in the same homotopy class.

Theorem 1 is now proven by contradiction. Suppose there exists a state $\mathbf{x}$, denoted as $\mathbf{x}^*$, along π^* (where π^* is the optimal path) that is *not included* in the greedy informed set $\mathcal{X}_{\hat{f}_{\text{greedy}}}(\pi)$, i.e.,

$$\forall \mathbf{x} \in \mathcal{X}_{\text{free}},\ \exists \mathbf{x} \in \pi^* \quad \text{s.t.} \quad \mathbf{x} \notin \mathcal{X}_{\hat{f}_{\text{greedy}}}(\pi). \tag{12}$$

In this case, π^* must leave the ellipsoid at some point and re-enter it, since both the initial state $\mathbf{x}_I$ and the goal state $\mathbf{x}_G$ are inside $\mathcal{X}_{\hat{f}_{\text{greedy}}}(\pi)$. Consequently, there will be at least two intersection points between π^* and the boundary of $\mathcal{X}_{\hat{f}_{\text{greedy}}}(\pi)$. For simplicity, let the states $\mathbf{x}_1$ and $\mathbf{x}_2$ be the two intersection points, and $\mathbf{x}_3$ represent the state outside the hyperellipsoid.

Since both π and π^* are homotopic paths, the subpath $\pi^*_{\mathbf{x}_1\mathbf{x}_2\mathbf{x}_3}$ of π^* can be continuously deformed onto the subpath $\pi_{\mathbf{x}_1\mathbf{x}_2}$ of π without colliding with any obstacles (Lemma 2).

By Definition 9, the cost of the deformed geodesic subpath $\pi^*_{\mathbf{x}_1\mathbf{x}_2}$ is lower than the cost of the subpath $\pi^*_{\mathbf{x}_1\mathbf{x}_2\mathbf{x}_3}$:

$$c(\pi^*_{\mathbf{x}_1\mathbf{x}_2}) < c(\pi^*_{\mathbf{x}_1\mathbf{x}_2\mathbf{x}_3}). \tag{13}$$

Therefore, connecting directly to $\mathbf{x}_2$ is shorter than passing through $\mathbf{x}_3$. According to the definition of an optimal path, we know that any subpath of it must also be optimal [41]. However, by (13), the cost of π^* is higher than the cost of the deformed path $\pi_{\mathbf{x}_I\mathbf{x}_1\mathbf{x}_2\mathbf{x}_G}$. This implies that traversing through $\mathbf{x}_3$ incurs a higher cost compared to connecting directly from $\mathbf{x}_1$ to $\mathbf{x}_2$ along the ellipsoid, which contradicts the optimality of π^*. Thus, the initial assumption that $\mathbf{x}^*$ is not in the greedy informed set by (12) must be false and proves Theorem 1. Therefore, the greedy informed set $\mathcal{X}_{\hat{f}_{\text{greedy}}}(\pi)$ must include all the states along the optimal path π^* when π and π^* are in the same homotopy class. □

While Theorem 1 establishes that the optimal path is guaranteed to be included in the greedy informed set when it shares the same homotopy class as the current solution path, this does not hold when the paths are homotopically distinct. In fact, there are cases where the greedy informed set may fail to include the optimal path precisely because of differences in homotopy classes. This leads us to explore scenarios where the optimal path is excluded from the greedy informed set (Theorem 2).

Theorem 2 (Scenarios where the greedy informed set does not contain the optimal path)**.** *There exist scenarios in which the greedy informed set $\mathcal{X}_{\hat{f}_{greedy}}$ does not contain the optimal path π^* due to their being in different homotopy classes.*

Proof. This proof is based on a counterexample and follows directly from Theorem 1. Consider a planning problem scenario in a maze-like environment with many homotopy classes between the initial state $\mathbf{x}_I$ and the goal state $\mathbf{x}_G$, as illustrated in Figure 6. Let π_i be a feasible path that follows a narrow corridor, navigating through obstacles by making several sharp turns. Let π^* be the optimal path in a different homotopy class, which avoids the narrow corridor. Instead, it circumvents the obstacles entirely, avoiding sharp turns. By construction, the greedy informed set is constrained by the geometry of the environment, specifically by the obstacles that force π_i through the narrow passage.

Since π_i and π^* belong to different homotopy classes, the path π_i cannot be continuously deformed into π^* without intersecting the obstacles (Lemma 1). Theorem 1 guarantees that the optimal path π^* will only be included in the greedy informed set if both π_i and π^* are homotopic. However, since $\mathcal{X}_{\hat{f}_{\text{greedy}}}$ is localized to states near the narrow passage, it excludes the optimal path π^*, which circumvents the obstacles. Therefore, in scenarios where the current feasible solution path and the optimal path belong to different homotopy classes, the greedy informed set may fail to capture the optimal path. □

This highlights the limitations of the greedy informed set in certain planning problems. When the optimal path belongs to a different homotopy class than the current solution path, the greedy informed set cannot guarantee the inclusion of the optimal path, which can lead to suboptimal performance.

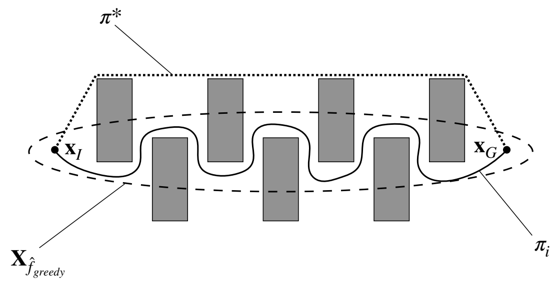

Fig. 6: Illustration of the sub-optimality of greedy informed set in an example planning scenario. The L^2 greedy informed set, $\mathcal{X}_{\hat{f}_{\text{greedy}}}$, highlighted in a dashed ellipse, is constructed based on the current tortuous solution path, π_i. The true optimal path, π^*, is depicted as a dotted line. Here, the greedy informed set does not contain all the vertices that can improve the current solution cost (i.e., those that contribute to approaching π^* and lie outside of the hyperellipsoid) due to the nature of its greedy exploitation.

Therefore, understanding this behavior is crucial, as it allows for the appropriate adjustment of the sampling rate from this set based on the distribution of homotopy classes and the type of planning problem being addressed. One effective approach to mitigate this issue is to also sample from the informed set with a certain probability (Section IV), which helps control the balance between exploration and exploitation within the planning algorithm.

IV. Greedy RRT* (G-RRT*)

Greedy RRT* is an almost surely asymptotically optimal path planning algorithm that builds on top of RRT*. Since it is an RRT*-like algorithm, it rapidly explores the problem domain by building a tree through obstacle-free space using random sampling. It also does the incremental rewiring of the growing tree to preserve the asymptotic optimality guarantees. However, rather than sampling randomly throughout the problem domain for the entire planning process, G-RRT* uses the direct informed sampling technique [12, 31] to focus the search on the promising regions of the state space once the initial solution is found. Specifically, it uses a greedy version of the informed set, introduced in Section III, to focus the search by exploiting knowledge of the existing solution path.

Finding a fast initial solution is important for G-RRT* to make use of all the benefits of informed sets, as RRT* and its informed variants behave the same until the initial solution is found. One way to accelerate this process is by utilizing bi-directional search, such as the bi-directional version of RRT [13] and its optimal variants [21, 42]. Therefore, G-RRT* improves the initial path finding time by leveraging the concepts of bi-directional search. It maintains two rapidly growing trees—one rooted at the start and one at the goal—to explore the problem's state space and uses a greedy connect heuristic to guide the trees toward each other, similar to RRT-Connect [13] algorithm. The complete algorithm is presented in Algorithms 1–5, with modifications to the bi-directional versions of RRT and RRT* variants highlighted in red.

Algorithm 1: Greedy RRT* $(\mathbf{x}_I, \mathbf{x}_G)$

$V_a \leftarrow \{\mathbf{x}_I\}; E_a \leftarrow \emptyset; G_a = (V_a, E_b);$
$V_b \leftarrow \{\mathbf{x}_G\}; E_b \leftarrow \emptyset; G_b = (V_b, E_b);$
$E_{\text{sol'n}} \leftarrow \emptyset;$
for $i = 1, \ldots, n$ **do**
  $c_{\text{i}} \leftarrow \text{ComputeBestCost}\,(E_{\text{sol'n}});$
  $\mathbf{x}_{\text{rand}} \leftarrow \text{Sample}\,(\mathbf{x}_I, \mathbf{x}_G, c_{\text{i}});$
  $\text{status}, \mathbf{x}_{\text{a}} \leftarrow \text{Extend*}\,(G_a = (V_a, E_a), \mathbf{x}_{\text{rand}});$
  if status $\neq$ TRAPPED **then**
    $\text{status}, \mathbf{x}_{\text{b}} \leftarrow \text{Connect*}\,(G_b = (V_b, E_b), \mathbf{x}_{\text{a}});$
    if status = REACHED **then**
      $E_{\text{sol'n}} \leftarrow E_{\text{sol'n}} \cup \{\mathbf{x}_{\text{a}}, \mathbf{x}_{\text{b}}\};$
  $\text{Swap}\,(G_a = (V_a, E_a), G_b = (V_b, E_b));$
return $G = (V_a \cup V_b, E_a \cup E_b);$

Algorithm 2: ComputeBestCost $(E_{\text{sol'n}} = \{(\mathbf{v}, \mathbf{w}) \mid \mathbf{v} \in V_a,\ \mathbf{w} \in V_b\})$

$c_{\text{i}} \leftarrow \infty;$
if $|X_{soln}| > 0$ **then**
  $c_{\text{i}} \leftarrow \min_{\mathbf{x} \in X_{\text{soln}}} \{g(\mathbf{x})\};$
  if $\epsilon > U\,([0, 1])$ **then**
    if $c_i < c_{min}$ **then**
      $c_{\text{min}} \leftarrow c_{\text{i}};$
      $c_{\text{max}} \leftarrow \max_{\mathbf{x} \in X_{\text{soln}}} \left\{\hat{f}(\mathbf{x})\right\};$
    $c_{\text{i}} \leftarrow c_{\text{max}};$
  else
    $c_{\text{min}} \leftarrow c_{\text{i}};$

Algorithm 3: Sample $(\mathbf{x}_I, \mathbf{x}_G, c_{\text{max}})$

repeat
  if $c_{max} < \infty$ **then**
    $\mathbf{x}_{\text{rand}} \leftarrow \text{SampleHyperEllipsoid}\,(\mathbf{x}_I, \mathbf{x}_G, c_{\text{max}});$
    if $\mathbf{x}_{rand} \in \mathcal{X} \cap \mathcal{X}_{PHS}$ **then**
      return $\mathbf{x}_{rand};$
  else
    $\mathbf{x}_{\text{rand}} \leftarrow \text{SampleUniform}\,(\mathcal{X});$
    return $\mathbf{x}_{rand};$
until $\mathbf{x}_{rand}$ *satisfies bounds*;

Algorithm 4: Extend* $(G = (V, E), \mathbf{x})$

$\mathbf{x}_{\text{nearest}} \leftarrow \text{Nearest}\,(G = (V, E), \mathbf{x});$
$\mathbf{x}_{\text{new}} \leftarrow \text{Steer}\,(\mathbf{x}_{\text{nearest}}, \mathbf{x});$
if *ObstacleFree* $(\mathbf{x}_{nearest}, \mathbf{x}_{new})$ **then**
  $V \leftarrow V \cup \{\mathbf{x}_{\text{new}}\};$
  $X_{\text{near}} \leftarrow \text{Near}\,(G = (V, E), \mathbf{x}_{\text{new}}, r_{\text{rewire}});$
  $\mathbf{x}_{\text{min}} \leftarrow \mathbf{x}_{\text{nearest}};$
  foreach $\mathbf{x}_{near} \in X_{near}$ **do**
    $c_{\text{near}} \leftarrow g(\mathbf{x}_{\text{near}}) + d(\mathbf{x}_{\text{near}}, \mathbf{x}_{\text{new}});$
    if $c_{near} < g(\mathbf{x}_{min}) + d(\mathbf{x}_{min}, \mathbf{x}_{new})$ **then**
      if *ObstacleFree* $(\mathbf{x}_{near}, \mathbf{x}_{new})$ **then**
        $\mathbf{x}_{\text{min}} \leftarrow \mathbf{x}_{\text{near}};$
  $E \leftarrow E \cup \{\mathbf{x}_{\text{min}}, \mathbf{x}_{\text{new}}\};$
  foreach $\mathbf{x}_{near} \in X_{near}$ **do**
    if $g(\mathbf{x}_{new}) + d(\mathbf{x}_{new}, \mathbf{x}_{near}) < g(\mathbf{x}_{near})$ **then**
      if *ObstacleFree* $(\mathbf{x}_{new}, \mathbf{x}_{near})$ **then**
        $\mathbf{x}_{\text{parent}} \leftarrow \text{Parent}\,(\mathbf{x}_{\text{near}});$
        $E \leftarrow E \setminus \{(\mathbf{x}_{\text{parent}}, \mathbf{x}_{\text{near}})\};$
        $E \leftarrow E \cup \{(\mathbf{x}_{\text{new}}, \mathbf{x}_{\text{near}})\};$
  if $\mathbf{x}_{new} = \mathbf{x}$ **then**
    return REACHED, $\mathbf{x}_{new};$
  else
    return ADVANCED, $\mathbf{x}_{new};$
return TRAPPED, $\mathbf{x}_{new};$

Algorithm 5: Connect* $(G = (V, E), \mathbf{x})$

repeat
  $\text{status}, \mathbf{x}_{\text{new}} \leftarrow \text{Extend*}\,(G = (V, E), \mathbf{x});$
until status $\neq$ ADVANCED;

A. Notation

The state space of the path planning problem is denoted by $\mathcal{X} \in \mathbb{R}^n$, where $n \in \mathbb{N}$. States that are in collision with obstacles are represented by $\mathcal{X}_{\text{obs}} \subseteq \mathcal{X}$, while valid, collision-free states are denoted by $\mathcal{X}_{\text{free}} = \mathcal{X} \setminus \mathcal{X}_{\text{obs}}$. The notation $\mathbf{x} \in \mathcal{X}$ represents a single state in the state space. The initial and goal states of the planning problem are denoted by $\mathbf{x}_I \in \mathcal{X}_{\text{free}}$ and $\mathbf{x}_G \in \mathcal{X}_{\text{free}}$, respectively.

A tree $G = (V, E)$ is defined by a set of vertices V and edges E. The start tree is denoted by $G_a = (V_a, E_a)$, and the goal tree is denoted by $G_b = (V_b, E_b)$. All vertices in the start and goal trees, V_a and V_b, are directly associated with the valid regions of the state space $\mathcal{X}_{\text{free}}$. Edges in both trees, $E \subset V \times V$, are directed and consist of a source vertex $\mathbf{v}$ and a target vertex $\mathbf{w}$, represented as $(\mathbf{v}, \mathbf{w})$.

The cost of the connection from the source vertex $\mathbf{v}$ to the target vertex $\mathbf{w}$ in the graph G is denoted by the scalar $c \in \mathbb{R}_{\geq 0}$, and its admissible heuristic is represented by $\hat{c} \in \mathbb{R}_{\geq 0}$, where $\forall v, w \in G$, $\hat{c}(\mathbf{v}, \mathbf{w}) \leq c(\mathbf{v}, \mathbf{w})$. The true cost of the optimal path from the initial vertex to a specific vertex $\mathbf{x}$, also called the cost-to-come of a vertex, is denoted by the function $g(\mathbf{x}) = c(\mathbf{x}_I, \mathbf{x})$, and its admissible estimate is $\hat{g}(\mathbf{x}) = \hat{c}(\mathbf{x}_I, \mathbf{x})$. The true cost of the optimal path from a vertex to the goal state, also called the cost-to-go of a vertex, is denoted by the function $h(\mathbf{x}) = c(\mathbf{x}, \mathbf{x}_G)$, and its admissible estimate is $\hat{h}(\mathbf{x}) = \hat{c}(\mathbf{x}, \mathbf{x}_G)$.

The summation of the two heuristic estimates, $\hat{g}(\mathbf{x})$ and $\hat{h}(\mathbf{x})$, defines the heuristic cost of the path from the start vertex $\mathbf{x}_I$, passing through a specific vertex $\mathbf{x}$, towards the goal vertex $\mathbf{x}_G$, i.e., $\hat{f}(\mathbf{x}) = \hat{g}(\mathbf{x}) + \hat{h}(\mathbf{x})$. This function, $\hat{f}(\mathbf{x})$, also defines the informed set, which is the set of states whose heuristic estimates can provide better solutions than the current solution cost (Definition 6). The vertex with the maximum admissible heuristic cost along the path from the start vertex to the goal vertex is denoted by $\mathbf{x}_{\text{max}}$. The function $\hat{f}(\mathbf{x}_{\text{max}})$ defines the greedy informed set, which is the set of states whose heuristic estimates can provide better solutions than the heuristic cost of this greedily chosen state, $\mathbf{x}_{\text{max}}$, in the current solution (Definition 7).

B. Greedy Informed Sampling

G-RRT* finds better solution paths to a planning problem by growing two trees, $G_a = (V_a, E_a)$ from the start and $G_b = (V_b, E_b)$ from the goal, consisting of the vertices $V_a \cup V_b$ and edges $E_a \cup E_b$, towards randomly sampled states in free space. These graphs are rewired with newly added vertices to minimize the cost-to-come for nearby vertices. Similar to Informed RRT*, once an initial solution is found, the algorithm focuses random sampling on a subset of the problem domain, constrained by admissible ellipsoidal heuristics, which accelerates convergence to the optimal solution. However, unlike Informed RRT*, which explores all states in the informed subset to improve the current solution cost, G-RRT* leverages information from the current solution path and biases random sampling toward a shrinking subset of the hyperellipsoid, known as the L^2 greedy informed set. It also samples from the informed exploration subset to maintain uniform distribution, ensuring asymptotic optimality. Specifically, G-RRT* balances the exploration and exploitation of the random sampling process by introducing a parameter, $\epsilon \in [0, 1]$, called the *greedy biasing ratio*. If $\epsilon = 0$, it only focuses the sampling on the informed subset, behaving the same as the Informed RRT* algorithm with pure exploration. On the other hand, if $\epsilon = 1$, the algorithm exploits the current solution path information and only finds the set of states within the greedy informed set with no exploration. Therefore, finding a good balance between uniform sampling for exploration and path-biased sampling for exploitation is necessary to rapidly reduce the size of the informed subset for faster convergence rates and global optimality guarantees.

At each iteration, G-RRT* finds the transverse diameter of the corresponding hyperellipsoids for the random sampling process (Alg. 1, Line 5; Alg. 2). First, it determines the current best cost, c_i, by calculating the cost required to reach the best goal vertex from the set of vertices in the goal region (Alg. 2, Lines 1–3). With probability ϵ, the algorithm computes the current maximum cost, c_{max}, for the sampling process by greedily selecting the best vertex along the existing solution path with the maximum admissible heuristic cost (i.e., exploitation using the L^2 greedy informed set) (Alg. 2, Lines 4–8). This greedy maximum cost is recalculated only when a new, better solution is found (Alg. 2, Line 5) to improve performance. With probability $1 - \epsilon$, the current best cost is defined by the solution cost computed in Alg. 2, Line 3 (i.e., exploration using the L^2 informed set), and the current minimum solution cost is cached for the next iteration (Alg. 2, Lines 9 and 10).

C. Tree Extension

Once a new random sample is found, G-RRT* performs the tree extension process similar to RRT-Connect by alternating between the two trees and connecting one tree toward the other repeatedly. First, the selected tree is extended from the nearest vertex, $\mathbf{x}_{\text{nearest}}$, toward $\mathbf{x}_{\text{rand}}$ using the Steer function, also known as a local planner, resulting in $\mathbf{x}_{\text{new}}$ (Alg. 1, Line 7; Alg. 4, Lines 1 and 2). If the resulting edge from $\mathbf{x}_{\text{nearest}}$ to $\mathbf{x}_{\text{new}}$ is valid, $\mathbf{x}_{\text{new}}$ is added to the set of vertices, V, of the current tree (Alg. 1, Line 7; Alg. 4, Lines 3 and 4). To achieve almost-sure asymptotic optimality, G-RRT* performs incremental tree rewiring in the local neighborhood of the newly added vertex, $\mathbf{x}_{\text{new}}$, as in RRT*. Once $\mathbf{x}_{\text{new}}$ is added to the tree, G-RRT* searches for the best potential parent vertex for this newly added state by considering the cost-to-come to nearby vertices within the local neighborhood radius (Alg. 1, Line 7; Alg. 4, Line 5). If connecting to a vertex from this set of candidate parents reduces the current cost-to-come to $\mathbf{x}_{\text{new}}$ and the edge is valid, the edge from the best parent vertex, $\mathbf{x}_{\text{min}}$, to $\mathbf{x}_{\text{new}}$ is added to the set of edges, E, in the current tree (Alg. 1, Line 7; Alg. 4, Lines 6–12).

If connecting to the new vertex, $\mathbf{x}_{\text{new}}$, can lower the cost-to-come of nearby vertices, they are rewired to become descendants of this vertex, provided the new edge is collision-free (Alg. 1, Line 7; Alg. 4, Lines 13–18). Similar to the RRT-Connect algorithm, the tree extension process in G-RRT* results in three possible outcomes: REACHED, if the newly generated vertex, $\mathbf{x}_{\text{new}}$, reaches the input vertex $\mathbf{x}$ (Alg. 1, Line 7; Alg. 4, Lines 19 and 20), ADVANCED, if $\mathbf{x}_{\text{new}} \neq \mathbf{x}$ is added to the vertex set (Alg. 1, Line 7; Alg. 4, Lines 21 and 22) and TRAPPED, if the edge from $\mathbf{x}_{\text{nearest}}$ to $\mathbf{x}_{\text{new}}$ is in collision (Alg. 1, Line 7; Alg. 4, Line 23).

D. Greedy Connect Heuristic

Certain planning problems are extremely challenging for planners to solve, particularly when either the start or goal states (or both) are obstructed by enclosures or narrow passages (as in Figures 7b and 7c). This difficulty increases as the dimensionality of the state space grows, making RRTs impractical for higher-dimensional applications. In our work, we address this challenge by utilizing a bi-directional search, maintaining two separate RRT trees at the start and goal states, respectively. In each iteration, while one tree is extended toward a randomly generated state using the EXTEND* procedure (Section IV-C), G-RRT* attempts to connect the newly added vertex to a nearby vertex from the other tree using a greedy CONNECT heuristic, similar to the RRT-Connect algorithm. It then alternates between these steps by swapping the two trees. This approach enables G-RRT* to quickly find paths in these challenging situations by leveraging the uniform explorative nature of RRTs to avoid local minima pitfalls while also exploiting a greedy strategy to connect the two trees.

Once the tree extension process toward the randomly generated vertex succeeds, G-RRT* attempts to extend the other tree toward the newly added vertex of the current tree using the greedy CONNECT* heuristic (Alg. 1, Lines 8–9). This process iteratively calls EXTEND* until the other tree either reaches the newly added vertex or fails to extend further due to a collision along the edge (Alg. 5). If this connection succeeds, meaning the other tree successfully connects to the newly added vertex of the current tree, a solution path is found, and this edge is added to the solution edge set $E_{\text{sol'n}}$, which maintains all the edges connecting the two trees (Alg. 1, Lines 10 and 11). To ensure both trees grow toward each other greedily, G-RRT* swaps the two trees before proceeding to the next iteration of the algorithm (Alg. 1, Line 12).

V. Analysis

A. Probabilistic completeness

A path planning algorithm is considered *robustly feasible* if there exists a solution path with strong δ-clearance (i.e., a distance δ away from any obstacle in $\mathcal{X} \in \mathbb{R}^n$) for some $\delta > 0$ [8]. An algorithm for solving any robustly feasible planning problem $(\mathcal{X}_{\text{free}}, \mathbf{x}_I, \mathbf{x}_G)$ has *probabilistic completeness* guarantees if there exists a goal vertex $\mathbf{x}_G$ in the graph where a start vertex $\mathbf{x}_I$ becomes connected to $\mathbf{x}_G$ as the number of samples approaches infinity (Definition 3). In other words, the algorithm is said to be probabilistically complete, if given sufficient time, it can find a solution to the path planning problem if one exists.

G-RRT* maintains two rapidly growing trees, each of which fulfills the probabilistic completeness property of classical RRTs. This means that during the alternating extension process of each RRT tree, new vertices are added to the sets V_a and V_b of start and goal trees where $V_k = V_a \cup V_b$ approaches $\mathcal{X}$ in probability with V_k being the set of RRT vertices after iteration k. Since the greedy CONNECT heuristic generates all the typical RRT vertices along with additional ones, it aids in covering $\mathcal{X}_{\text{free}}$, and therefore does not adversely affect the convergence results.

B. Asymptotic optimality

Consider a robustly feasible path planning problem defined by the state space $\mathcal{X}_{\text{free}}$, initial state $\mathbf{x}_I$, and goal state $\mathbf{x}_G$, we define the optimal path planning problem as to find a path π^* from $\mathbf{x}_I$ to $\mathbf{x}_G$ that minimizes a cost function $c : \Sigma \to \mathbb{R}_{\geq 0}$ where Σ is the set of all feasible paths (Definition 2). A solution path π^* is considered robustly optimal if there exists another path π_0 with strong δ-clearance in the same homotopy class where $c(\pi_0) = \min\{c(\pi) : \pi \text{ is feasible}\}$ [8]. A solution path π^* is considered *asymptotically optimal* if, for any robustly feasible planning problem $(\mathcal{X}_{\text{free}}, \mathbf{x}_I, \mathbf{x}_G)$ and cost function $c : \Sigma \to \mathbb{R}_{\geq 0}$ that produces a robustly optimal solution, the following holds:

$$P(\limsup_{n\to\infty} Y_n = c^*) = 1 \tag{14}$$

where $Y_n \geq c^*, \forall n \in \mathbb{N}$ is the cost of the best solution found in the graph G at the end of iteration n and c^* is the theoretical minimum cost (Definition 4).

RRT* has proven to be asymptotically optimal by incrementally rewiring the tree around new vertices [8]. These are the set of vertices which are within the n-dimensional unit ball of radius, r_{rewire}, of the newly added vertex in the Euclidean space:

$$r_{rewire} = \min\{\eta, r_{\text{RRT*}}\} \tag{15}$$

where $\eta > 1$ represents the maximum adjustable edge length of the tree, while $r_{\text{RRT*}}$ is a function that depends on the problem measure and the number of vertices in the current tree. Here,

$$r_{\text{RRT*}} := \left(2\left(1+\frac{1}{n}\right)\left(\frac{\lambda(\mathcal{X}_{\text{free}})}{\zeta_n}\right)\left(\frac{\log(|V|)}{|V|}\right)\right)^{\frac{1}{n}} \tag{16}$$

where $\lambda(\cdot)$ denotes the Lebesgue measure of a set, ζ_n represents the Lebesgue measure of an n-dimensional unit ball, $|\cdot|$ indicates the cardinality of a set, with n denoting the number of dimensions in the state space.

Direct informed sampling approaches have also shown to be maintaining the property of asymptotic optimality of RRT* however they only search on a subset of the original planning problem [12, 31]. Therefore, this reduces the computational requirements of rewiring at each planning iteration due to the smaller number of rewiring neighborhoods. Here, the rewiring requirements to maintain the asymptotic optimality in the smaller subset of the planning domain is a function of the number of vertices in the informed set, $|V \cap \mathcal{X}_{\hat{f}}|$, and its measure, $\lambda(\mathcal{X}_{\hat{f}})$.

G-RRT* uses the greedy informed set $\mathcal{X}_{\hat{f}_{\text{greedy}}}$ described in Section III to focus the search on even smaller subset of the planning domain than the informed set, where, it is bounded from above by the informed subset, i.e., $\mathcal{X}_{\hat{f}_{\text{greedy}}} \supseteq \mathcal{X}_{\hat{f}}$. This increases the chances of finding the vertices that are more likely to be inside the omniscient set (Definition 5), improving the rate of converging to the optimal solution. Here, the rewiring requirements of G-RRT* is a function of the number of vertices in the greedy informed set, $|V \cap \mathcal{X}_{\hat{f}_{\text{greedy}}}|$, and its measure, $\lambda(\mathcal{X}_{\hat{f}_{\text{greedy}}})$ where

$$r_{\text{G-RRT*}} := \left(2\left(1+\frac{1}{n}\right)\left(\frac{\lambda\left(\mathcal{X}_{\hat{f}_{\text{greedy}}}\right)}{\zeta_n}\right)\left(\frac{\log(|V \cap \mathcal{X}_{\hat{f}_{\text{greedy}}}|)}{|V \cap \mathcal{X}_{\hat{f}_{\text{greedy}}}|}\right)\right)^{\frac{1}{n}}. \tag{17}$$

However, not all vertices in the greedy informed set are guaranteed to be in the omniscient set as it is an overly approximated version of it which may or may not be an upper bound estimate of the true omniscient set (see Figure 6). In other words, vertices that could lead to better solution paths may exist outside the homotopy regions of the greedy informed set (Theorem 2). Since G-RRT* also samples from the informed subset based on the greedy biasing ratio (Section IV-B), it still holds the asymptotic optimality guarantees of direct informed sampling techniques.

This raises the question of how sampling with the greedy informed set affects the worst-case number of samples required for probabilistic optimality. Theorem 3 quantifies this impact by comparing it to sampling with the informed set only.

Theorem 3 (Impact on the worst-case number of samples for probabilistic optimality)**.** *The worst-case number of samples required for probabilistic optimality using the greedy informed set grows proportionally by a factor of $\frac{1}{1-\epsilon}$ compared to using only the informed set.*

Proof. Let $P(\mathbf{x}_{\text{rand}} \in \mathcal{X}_f)$ represent the probability of sampling a state from the omniscient set. According to Lemma 5 from [31], sampling states from the omniscient set is a necessary condition for improving the current solution in RRT*-like algorithms. Let $P(\mathbf{x}_{\text{rand}} \in \mathcal{X}_{\hat{f}})$ represent the probability of sampling a state from the informed set. Since $\mathcal{X}_{\hat{f}} \supseteq \mathcal{X}_f$, as noted in [31], sampling from the informed set is also a necessary condition for probabilistic optimality, and its probability is bounded below by the probability of sampling from $\mathcal{X}_f$:

$$P(\mathbf{x}_{\text{rand}} \in \mathcal{X}_f) \leq P(\mathbf{x}_{\text{rand}} \in \mathcal{X}_{\hat{f}})$$

Thus, the expected number of samples required to improve the current solution to a holonomic problem depends on the probability of sampling the informed set, and is given by:

$$E[n] = \frac{1}{P(\mathbf{x}_{\text{rand}} \in \mathcal{X}_{\hat{f}})} \tag{18}$$

Recall that with probability $1-\epsilon$, we sample from the informed set, and with probability ϵ, we sample from the greedy informed set. Therefore, the overall probability of sampling from $\mathcal{X}_{\hat{f}}$ in any given iteration is reduced, since we do not always sample from $\mathcal{X}_{\hat{f}}$. Specifically, the new probability $P_{\text{new}}(\mathbf{x}_{\text{rand}} \in \mathcal{X}_{\hat{f}})$ of selecting a random sample from $\mathcal{X}_{\hat{f}}$ is:

$$P_{\text{new}}(\mathbf{x}_{\text{rand}} \in \mathcal{X}_{\hat{f}}) = (1-\epsilon) \cdot P(\mathbf{x}_{\text{rand}} \in \mathcal{X}_{\hat{f}}) \tag{19}$$

Substituting (19) into (18), the expected number of samples required to sample from $\mathcal{X}_{\hat{f}}$ now becomes:

$$\begin{aligned} E[n_{\text{new}}] &= \frac{1}{P_{\text{new}}(\mathbf{x}_{\text{rand}} \in \mathcal{X}_{\hat{f}})} \\ &= \frac{1}{(1-\epsilon) \cdot P(\mathbf{x}_{\text{rand}} \in \mathcal{X}_{\hat{f}})} \end{aligned} \tag{20}$$

Comparing (18) and (20):

$$\frac{E[n_{\text{new}}]}{E[n]} = \frac{\frac{1}{(1-\epsilon)\cdot P(\mathbf{x}_{\text{rand}} \in \mathcal{X}_{\hat{f}})}}{\frac{1}{P(\mathbf{x}_{\text{rand}} \in \mathcal{X}_{\hat{f}})}} = \frac{1}{1-\epsilon}$$

Therefore, in the worst case where the greedy informed set does not include states from the optimal solution, the number of samples required for asymptotic optimality increases by a factor of $\frac{1}{1-\epsilon}$ compared to only sampling from $\mathcal{X}_{\hat{f}}$. □

VI. Simulation and Experiments

Greedy RRT* was compared against the Open Motion Planning Library (OMPL) [43] implementations of RRT-Connect, RRT*, Informed RRT*, RRT*-Connect [21], BIT* [44] and AIT* [45, 46] on simulated planning problems in $\mathbb{R}^2$, $\mathbb{R}^4$, $\mathbb{R}^8$ and $\mathbb{R}^{16}$ (Section VI-A), manipulation problems for two Barret WAM arms with 14 degrees-of-freedom ($\mathbb{R}^{14}$) in the Open Robotics Automation Virtual Environment (OpenRAVE) [47] (Section VI-B) and real-world planning problem for a self-reconfigurable mobile robot Panthera in SE(2) and SE(2) + $\mathbb{R}^2$ state spaces (Section VI-D)[1]. Planner developer tools (PDT) [48] was used to run all the experiments.

[1]Simulations were run in Ubuntu 22.04 docker container on a MacBook Air with 16 GB of RAM and Apple M2 chip.

The planners were tested with the optimization objective of minimizing path length. All the planners used maximum edge lengths of 0.3, 0.4, 0.5, 0.65, 1.25, 2.4 and 3.0 in $\mathbb{R}^2$, SE(2), $\mathbb{R}^4$, SE(2) + $\mathbb{R}^2$, $\mathbb{R}^8$, $\mathbb{R}^{14}$ and $\mathbb{R}^{16}$, respectively. An RGG constant of $\eta = 1.001$ was used for all the planners, and the Euclidean distance (i.e., L^2 norm) for path length was used as an admissible cost heuristic. The BIT*-based planners used a batch size of 100, and G-RRT* used a greedy biasing ratio of $\epsilon = 0.9$ to urge the exploitation in all the experiments.

A. Abstract planning problems

The planners were tested on three simulated planning problems in $\mathbb{R}^2$, $\mathbb{R}^4$, $\mathbb{R}^8$, and $\mathbb{R}^{16}$ as depicted in Figure 7. The first problem consists of many axis-aligned homotopy classes and/or (hyper)rectangles, filled over the whole problem state space, where the initial and goal states are located at $[-0.25, 0.0, \ldots, 0.0]^T$ and $[0.25, 0.0, \ldots, 0.0]^T$, respectively (Figure 7a). The second problem contains two homotopy classes with a narrow passage gap of width 0.04, where the initial and goal states are located at $[-0.3, 0.0, \ldots, 0.0]^T$ and $[0.3, 0.0, \ldots, 0.0]^T$, respectively (Figure 7b). The last experiment is a challenging dual-enclosure problem from planning literature, consisting of two hollow axis-aligned (hyper)rectangles enclosing the initial and goal states. Here, the initial and goal states are located at $[-0.3, 0, \ldots, 0]^T$ and $[0.3, 0, \ldots, 0]^T$, respectively (Figure 7c). Note that the planning time given to the planners varies based on the difficulty of the problem domain and the number of state dimensions. Each planner was run 100 trials with different pseudorandom seeds in which the solution cost was recorded every 10^{-4} seconds by a separate thread. If the solution is not found yet during recording, we set the value of a solution cost to be infinity for the purpose of calculating the median. Figures 8, 9 and 10 present the performance of the tested planners on these planning problems, where the median solution cost of each planner, together with its success rate, is plotted versus computation time.

These results demonstrate the necessity of exploitation in sampling-based planners for tackling challenging planning problems. G-RRT* performs comparably to AIT* and BIT* in lower state dimensions and consistently outperforms all other RRT*-based algorithms. It finds solutions in every trial, achieving a 100% success rate, and is competitive with the RRT-Connect algorithm in terms of success rate. In higher dimensions, G-RRT* outperforms all the anytime sampling-based planners, particularly in converging to optimal solutions.

From the results, we can observe that the performance of the RRT-based planners decreases as the state dimension grows. These single-tree planners struggle to find solutions within the available planning time, especially in $\mathbb{R}^{16}$, as shown in the experiments from Figures 7a and 7b. Note that we omitted running the single-tree RRT versions in the double enclosures experiment (Figure 7c) since it is a highly challenging problem, widely recognized as a *bug trap* problem for any sampling-based planning algorithm in high dimensions [49].

1) Problems with axis-aligned homotopy classes: In this problem involving many axis-aligned homotopy classes (Figure 7a), there is not much difference in performance between

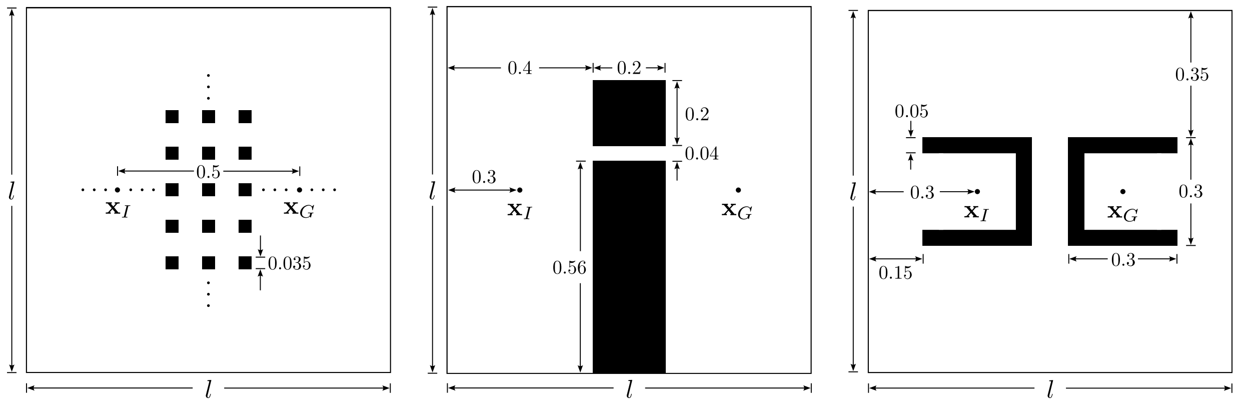

(a) (b) (c)

Fig. 7: Illustrations of the simulation experiments on which the planners were tested. These include complex planning problems containing (a) many homotopy classes, (b) narrow passage gap environment and (c) double enclosures with a problem domain of size $l = 1$. The $\mathbf{x}_I$ and $\mathbf{x}_G$ represent the initial and goal states respectively.

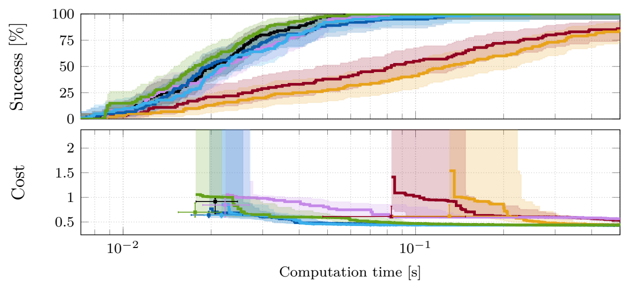

(a) Many homotopy classes in $\mathbb{R}^2$

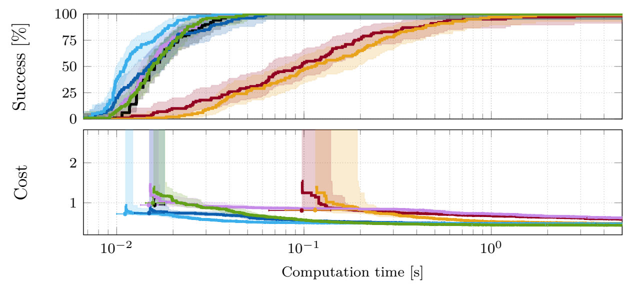

(b) Many homotopy classes in $\mathbb{R}^4$

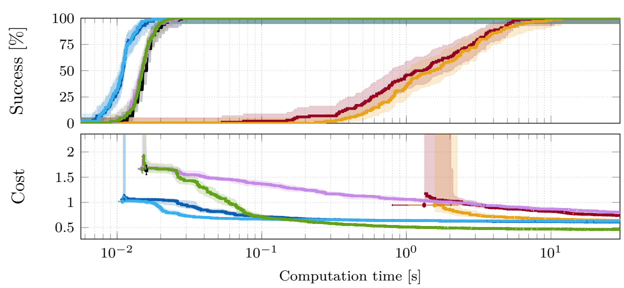

(c) Many homotopy classes in $\mathbb{R}^8$

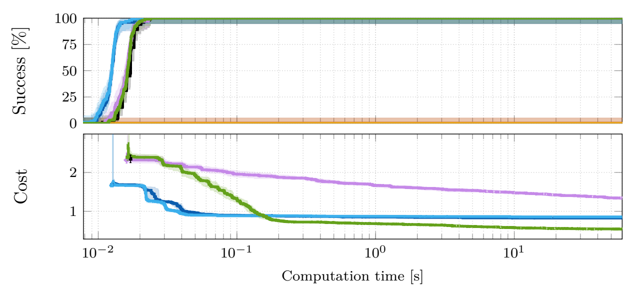

(d) Many homotopy classes in $\mathbb{R}^{16}$

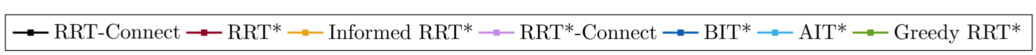

Fig. 8: Planner performance versus running time on the many homotopy classes problem described in Section VI-A (Figure 7a). The success plots represent the percentage of number of successful runs over time and the cost plots show the median solution cost versus run time for each planner. The error bars and shaded areas denote non-parametric 99% confidence intervals on the median. Each planner was run for 100 trials with running times of 0.5, 5.0, 30.0 and 100.0 seconds in $\mathbb{R}^2$, $\mathbb{R}^4$, $\mathbb{R}^8$ and $\mathbb{R}^{16}$, presented in plots (a), (b), (c) and (d), respectively.

the planners in $\mathbb{R}^2$ and $\mathbb{R}^4$ (Figures 8a and 8b). Here, G-RRT*, BIT*, AIT*, and RRT-Connect find solutions faster than other RRT*-based planners with a similar success rate. However, as the state dimension grows—i.e., in $\mathbb{R}^8$ and $\mathbb{R}^{16}$, G-RRT* outperforms all the tested planners in converging to the lowest cost in a shorter time period, followed by BIT* and AIT* algorithms (Figures 8c and 8d). Note that in $\mathbb{R}^{16}$ problems, RRT*-based planners are not able to find solutions within the available time budget.

2) Narrow passage gap problems: In this experiment involving a narrow passage gap (Figure 7b), all the tested planners were able to find solutions in $\mathbb{R}^2$ and $\mathbb{R}^4$ problems with a 100% success rate (Figures 9a and 9b). Here, G-RRT*, BIT*, and AIT* planners converge to the optimum at a similar rate when finding a solution through a narrow passage gap. However, RRT*-based algorithms struggle to find a path

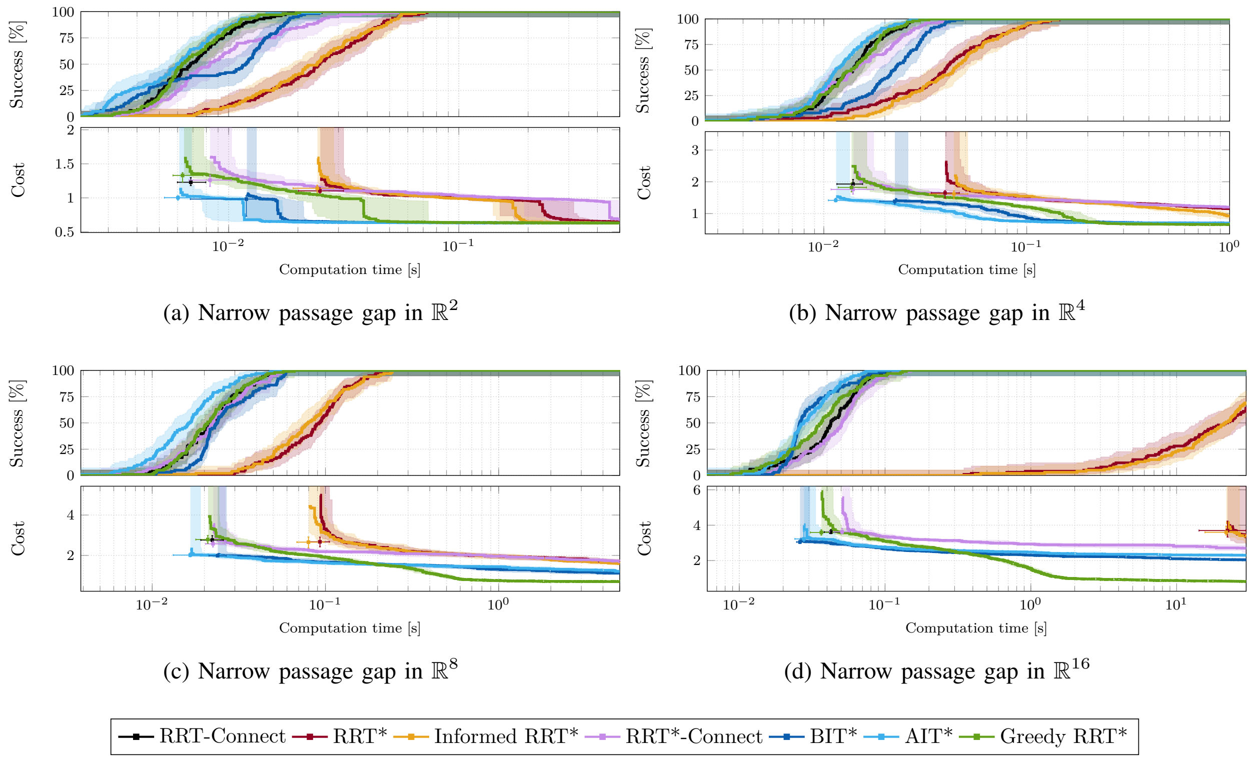

(a) Narrow passage gap in $\mathbb{R}^2$

(b) Narrow passage gap in $\mathbb{R}^4$

(c) Narrow passage gap in $\mathbb{R}^8$

(d) Narrow passage gap in $\mathbb{R}^{16}$

Fig. 9: Planner performance versus running time on the narrow passage gap problem described in Section VI-A (Figure 7b). The success plots represent the percentage of number of successful runs over time and the cost plots show the median solution cost versus run time for each planner. The error bars and shaded areas denote non-parametric 99% confidence intervals on the median. Each planner was run for 100 trials with running times of 0.5, 1.0, 5.0 and 30.0 seconds in $\mathbb{R}^2$, $\mathbb{R}^4$, $\mathbb{R}^8$ and $\mathbb{R}^{16}$, presented in plots (a), (b), (c) and (d), respectively.

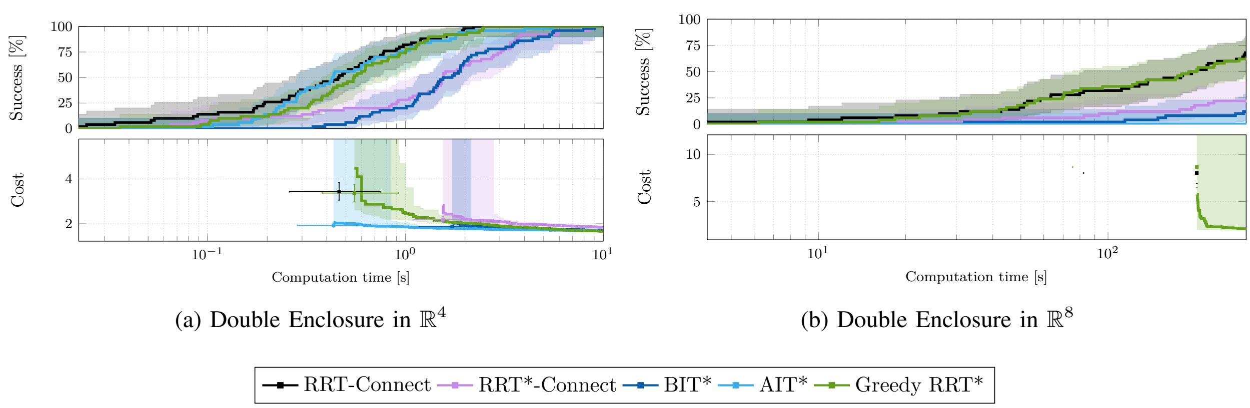

(a) Double Enclosure in $\mathbb{R}^4$

(b) Double Enclosure in $\mathbb{R}^8$

Fig. 10: Planner performance versus running time on the double enclosure problem described in Section VI-A (Figure 7c). The success plots represent the percentage of number of successful runs over time and the cost plots show the median solution cost versus run time for each planner. The error bars and shaded areas denote non-parametric 99% confidence intervals on the median. Each planner was run for 50 trials with running times of 10.0 and 300.0 seconds in $\mathbb{R}^4$ and $\mathbb{R}^8$, presented in plots (a) and (b), respectively.

through the narrow passage gap in $\mathbb{R}^4$. On the other hand, there is a noticeable performance change in higher state dimensions, such as $\mathbb{R}^8$ and $\mathbb{R}^{16}$ problems. All asymptotically optimal planners struggle to find a path through a narrow passage gap, but G-RRT* is the only planner that is able to find a path through it within the available time budget, and the difference becomes larger as the state dimension increases (Figures 9c and 9d).

3) Double enclosures problems: We also conducted experiments on challenging problems involving double enclosures symmetric around the start and goal states. Since all asymptotically optimal sampling-based planners struggled to solve this problem as state dimensions increased, it was only run for $\mathbb{R}^4$ and $\mathbb{R}^8$ problems, and RRT*-based planners were omitted from the experiments. In $\mathbb{R}^4$, all the tested planners

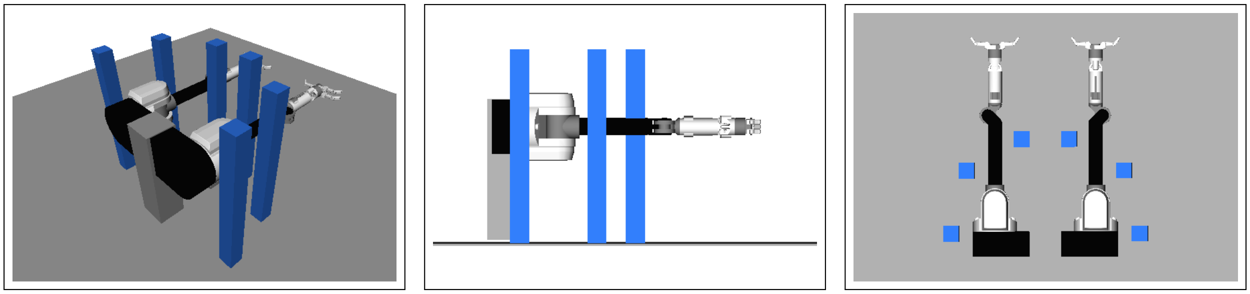

(a) Start configuration (b) Start configuration (side view) (c) Start configuration (top view)

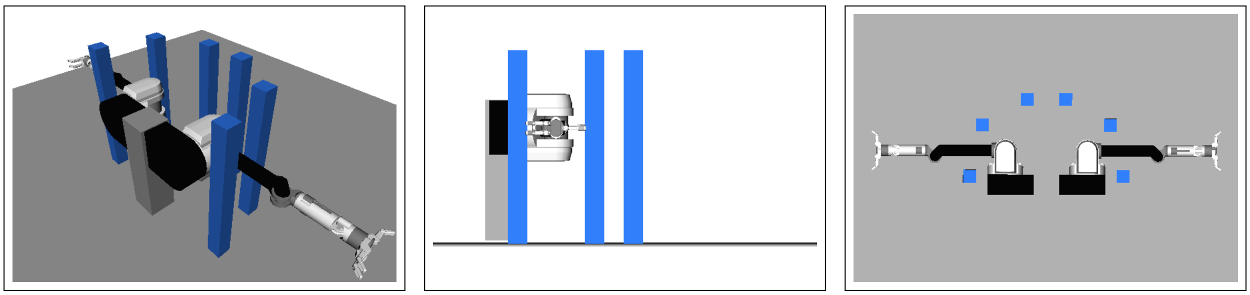

(d) Goal configuration (e) Goal configuration (side view) (f) Goal configuration (top view)

Fig. 11: A dual-arm manipulation problem for the Barrett WAM Arm in $\mathbb{R}^{14}$. Starting from the configuration of the arms pointing in the same direction (a-c), the arms must be moved to extend outward in opposite directions without hitting the cage (d-f).

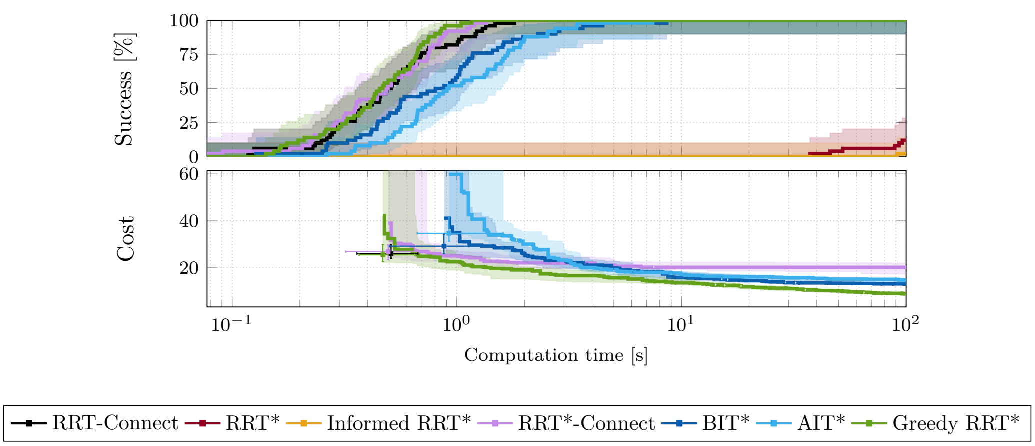

Fig. 12: Planner performance versus running time on the manipulation experiment described in Section VI-B (Figure 11). The success plots represent the percentage of a number of successful runs over time and the cost plots show the median solution cost versus run time for each planner. The error bars and shaded areas denote non-parametric 99% confidence intervals on the median. Each planner was run for 50 trials with running time of 100.0 seconds in $\mathbb{R}^{14}$.

were able to solve the problem within the available time and showed comparable performance in converging to the optimum (Figure 10a). However, all asymptotically optimal planners struggled to solve this problem in higher state dimensions, specifically in $\mathbb{R}^8$. G-RRT* and RRT-Connect were the only planners that found a solution in more than 50% of the trials (Figure 10b). This demonstrates the importance of maintaining two greedily connecting trees in problems involving several biased Voronoi regions [49]. Nevertheless, since RRT-Connect is a non-anytime planner that cannot converge to the optimum, G-RRT* is the only almost-surely asymptotically optimal planner that requires less time to find better median solution costs within an available planning time in higher state dimensions.

B. Manipulation Problems

The planners were also tested on manipulation tasks involving Barrett Whole-Arm Manipulator (WAM) arms within the Open Robotics Automation Virtual Environment (OpenRAVE) [47]. OpenRAVE was set up to utilize the Flexible Collision Library (FCL) [50], with a collision checking resolution set at 10^{-2}. Figure 11 depicts the dual-arm planning experiment for two Barrett WAM arms with 14 degrees-of-freedom. The objective is to move them from an initial configuration, where they point in the same forward direction, to a goal configuration where the arms are extended outward in opposite directions without colliding with the cage. Results for the performance of all the tested algorithms when optimizing path length are illustrated in Figure 12.

From the results, it is evident that RRT* and Informed RRT* planners struggle to find solutions within the available planning time due to the high dimensionality of state spaces. In contrast, G-RRT* quickly finds initial solutions, as fast as RRT-Connect and RRT*-Connect algorithms, all achieving a 100% success rate, followed by BIT* and AIT*. In summary, G-RRT* outperforms all tested asymptotically optimal planners in converging to optimal solutions, while also matching the speed of non-optimal planners in finding initial solutions.

C. Effect of greedy biasing ratio on convergence rate

In this section, we investigate how varying the greedy biasing ratio ϵ influences the convergence rate, exploitation vs. exploration balance, and the overall solution quality for different types of planning problems in both low and high-dimensional spaces. We experiment with values of 0, 0.5, 0.9, and 1.0 to represent a spectrum from pure exploration to pure exploitation. At $\epsilon = 0$, the planner performs fully informed sampling, focusing on exploration. As epsilon increases, the planner shifts toward greedy informed sampling, with $\epsilon = 1.0$ representing complete exploitation.

To assess the impact of the greedy biasing ratio on convergence, we evaluate the single-tree-based RRT* algorithm with greedy informed sampling, varying the ϵ values. These variants are applied to the abstract planning problems introduced in Section VI-A, focusing on $\mathbb{R}^2$, $\mathbb{R}^4$, and $\mathbb{R}^8$ spaces. We exclude $\mathbb{R}^{16}$ due to the difficulty single-tree planners face in finding initial solutions in high-dimensional spaces. For similar reasons, only $\mathbb{R}^2$ and $\mathbb{R}^4$ spaces are considered for the double enclosure problems.

Figure 13 presents the greedy exploitation effect across different planning problems and state dimensions. Planners using $\epsilon = 0.9$ and $\epsilon = 1.0$ outperform all other variants in converging faster to the optimum, followed by the planner using $\epsilon = 0.5$ (i.e., half exploration with the informed set and half exploitation with the greedy informed set). When $\epsilon = 0.0$ is used (i.e., full exploration with the informed set), it struggles to converge to the optimal solution, and this gap becomes larger as the difficulty of the planning problem increases. Notably, planners using $\epsilon = 0.9$ and $\epsilon = 1.0$ show similar behavior across all problems, regardless of state dimensions.

This demonstrates that an ϵ value of 0.9 is sufficient to significantly improve the convergence rate of planning algorithms using direct sampling procedures. The remaining 10% chance also preserves optimality due to the likelihood of correctly sampling the omniscient set by sampling the informed set, which is a necessary condition to improve the current solution to a holonomic problem (Lemma 12, [31]). In practice, however, this difference can be ignored, and using $\epsilon = 1.0$ will still lead to convergence and preserve optimality, though there is a risk of getting stuck in local minima in certain planning problems (see Theorem 2, Section III).

D. Planning for Panthera reconfigurable robot in real-world environment

We validate the proposed G-RRT* algorithm using a self-reconfigurable robot, Panthera, developed by [14] as a case study. Panthera has four independent steering units designed for omnidirectional locomotion. Its body frame can also be expanded and compressed by independently controlling two additional gaits to traverse tight spaces, as shown in Figure 14. The state of Panthera in the world frame can be represented as a 5-dimensional space, x, y, θ, j_0, j_1, where x, y, θ denotes the SE(2) state space, and j_0, j_1 are the two controllable gaits of Panthera in $\mathbb{R}^2$. Here, the angles for each steering unit of Panthera are not considered during planning, as this paper focuses only on geometric path planning. The resultant paths from the planners consist solely of waypoints representing the robot's state space, with an external local trajectory controller responsible for following these generated waypoints.

To evaluate the efficiency of trajectories generated from a predefined source to destination inside the real-world environment, the solution paths of G-RRT* were compared against Informed RRT* in both $\mathrm{SE}(2)$ (i.e., without reconfiguration) and $\mathrm{SE}(2) + \mathbb{R}^2$ state spaces (i.e., with reconfiguration) using the Panthera robot as a case study. G-RRT* and Informed RRT* are integrated into the navigation stack of the ROS framework [51] as global planner plugins. Once the global paths were generated to connect these waypoints, the robot followed the path within the prebuilt map, executing the velocity commands issued by a local trajectory controller to track the waypoints along the global path in an orderly manner. The local path planner used in this work is based on our previous study [52], which was also integrated into the ROS framework for Panthera. To enable reconfigurability, the robot's flexible base width was set as an adaptive footprint parameter in the global planning layer, with the configuration states adjusted at each waypoint according to the specific methods being tested. The experiments were conducted for 10 trials, and the solutions of G-RRT* and Informed RRT* were selected after 10 seconds of planning time for $\mathrm{SE}(2)$ and 30 seconds for $\mathrm{SE}(2)+\mathbb{R}^2$ to conduct the navigation experiments.

Using HDL 3D SLAM [53] with a 3D Velodyne 16-channel sensor, the 3D workspace was mapped, as shown in Figure 15. The workspace consists of several possible options (Path 1, 2, and 3, as seen in Figure 15) with different path lengths to connect the predefined source to destination waypoints. The example global path of each tested method is shown in Figure 16. Among the three path options in the tested map, both Informed RRT* and G-RRT* found a solution through path option 1 in the $\mathrm{SE}(2)$ state space (i.e., a 3-dimensional space without reconfiguration). In the $\mathrm{SE}(2) + \mathbb{R}^2$ state space (i.e., a 5-dimensional space with reconfiguration), both planners found a solution through path option 2, which involved a narrow passage. However, the paths generated by G-RRT* within the available time intervals were approximately 9% shorter and exhibited fewer twists and turns compared to those produced by Informed RRT*.

A smoother path allows the robot to follow the trajectory more easily, contributing to improved energy efficiency.

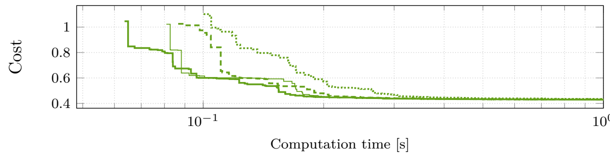

(a) Many homotopy classes in $\mathbb{R}^2$

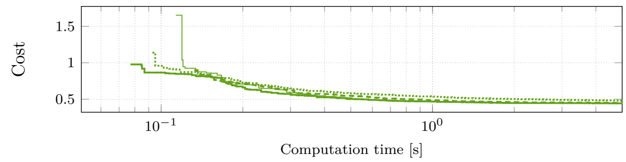

(b) Many homotopy classes in $\mathbb{R}^4$

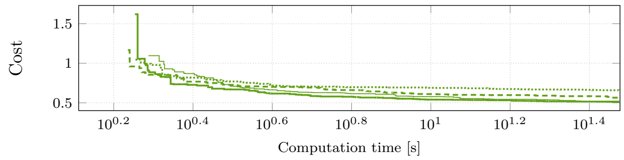

(c) Many homotopy classes in $\mathbb{R}^8$

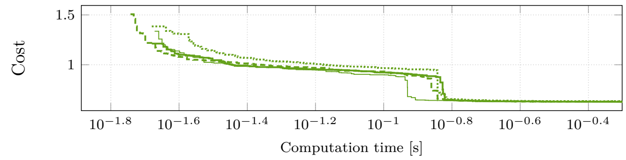

(d) Narrow passage gap in $\mathbb{R}^2$

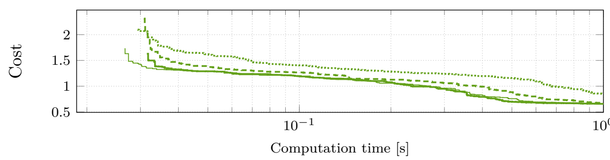

(e) Narrow passage gap in $\mathbb{R}^4$

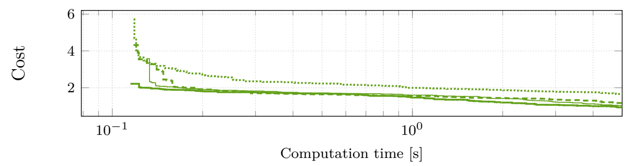

(f) Narrow passage gap in $\mathbb{R}^8$

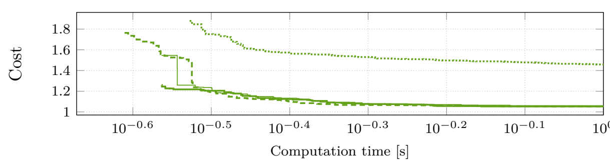

(g) Double Enclosure in $\mathbb{R}^2$

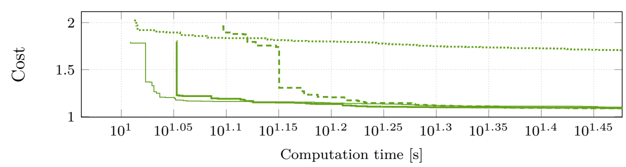

(h) Double Enclosure in $\mathbb{R}^4$

$\epsilon = 0.0$ $\epsilon = 0.5$ $\epsilon = 0.9$ $\epsilon = 1.0$

Fig. 13: Effect of varying greedy biasing ratios on the planner's convergence rate for the experiment described in Section VI-C. The plots show the median solution cost versus running time for the abstract planning problems outlined in Section VI-A. In these experiments, RRT* was modified to incorporate greedy informed sampling, using biasing ratio values of 0, 0.5, 0.9, and 1.0. Each variation was tested over 100 trials in $\mathbb{R}^2$, $\mathbb{R}^4$, and $\mathbb{R}^8$ for problems involving many homotopy classes and narrow passage gap (plots a-f) and in $\mathbb{R}^2$ and $\mathbb{R}^4$ for the double enclosure problem (plots g-h).

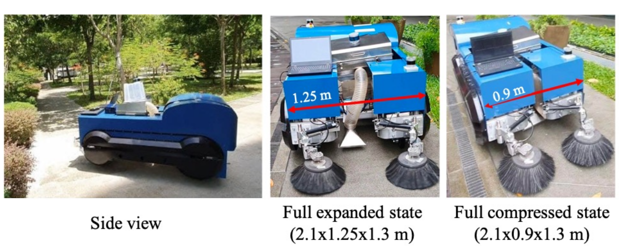

Fig. 14: Panthera reconfigurable pavement-sweeping platform with the ability to expand and compress.

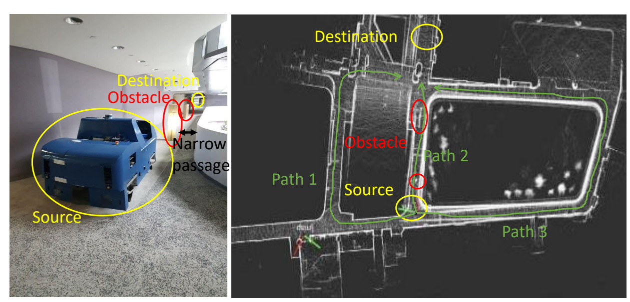

Fig. 15: The workspace setup of the real environment.

Hence, in addition to path length, numerical comparisons between G-RRT* and Informed RRT* also considered the time spent and energy consumption during navigation. Energy consumption data were obtained from Panthera's battery management system, with the current sampled at 10 kHz at 48 V. The maximum motor speed during the experiments was 150 rpm. By integrating these current measurements over time, the total energy consumption can be calculated while the robot navigates the path. The average energy consumption and navigation time after 10 trials are presented in Table I. We can observe that G-RRT* outperforms Informed RRT* in terms of both energy usage and time spent, with the margins of outperformance being significantly larger in higher-dimensional state spaces. Specifically, in the case of a 3-dimensional space without reconfiguration, the time and energy spent by Informed

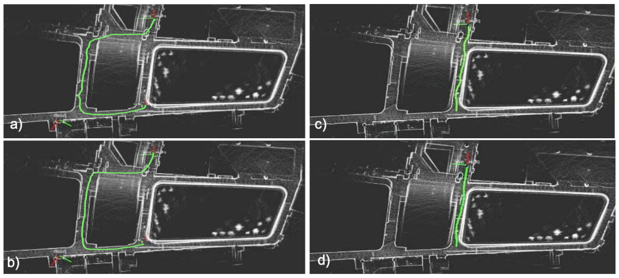

Fig. 16: The robot navigation trajectories (in green) in the 3D map of the real testbed workspace. (a) Informed RRT* without reconfiguration, (b) G-RRT* without reconfiguration, (c) Informed RRT* with reconfiguration, and (d) G-RRT* with reconfiguration.

TABLE I: Execution time and energy consumption of the planners for the real-world testbed environment.

planners	without reconfiguration		with reconfiguration	
	running time (s)	energy consumption (kJ)	running time (s)	energy consumption (kJ)
Infomed RRT*	632.25	151.2	372.63	103.6
G-RRT*	592.59	139.9	311.68	92.2

RRT* are only slightly higher than those of the proposed method, G-RRT*, at about 6.69% and 8.08%, respectively. However, when the search space increases to 5 dimensions, considering the reconfiguration of Panthera during planning, Informed RRT* consumes significantly more time and energy than G-RRT*, as expected due to the increased complexity in finding optimal solutions. The difference in time and energy consumption for Informed RRT* in this case increases to 19.56% and 12.36%, respectively, resulting in a trajectory with more turns and less smoothness.

VII. Conclusion and Discussion

Anytime sampling-based planning algorithms have been proven to perform better in high-dimensional state spaces compared to graph-search approaches since these methods do not explicitly construct high-dimensional occupancy obstacles; instead, they rely on random sampling to asymptotically find optimal solutions. Algorithms like RRT* increasingly build dense approximations over the problem domain based on randomly sampled states and find continually improving solutions over time. This makes RRT* probabilistically complete and almost-surely asymptotically optimal [18].

Although they are effective in continuous planning problems, their search is often inefficient since they tend to uniformly explore the entire state space (i.e., they are space-filling algorithms). In other words, these algorithms tend to spend time exploring unnecessary regions of the problem domain where solutions do not exist. This wasted computational effort becomes more significant in planning problems with higher dimensions of state space.

Previous studies therefore attempt to focus the search solely on promising regions of the problem domain where solutions are likely to exist. Algorithms such as Informed RRT* directly focus sampling on a subset of the state space determined by the current solution path. This L^2 informed set contains the set of states that can potentially provide better solutions and often ensures faster convergence guarantees for planning scenarios aimed at minimizing path lengths. However, since this set is estimated using the cost of the current solution path, it can still result in larger sampling regions, especially when the current solution contains many twists and turns.

We present an alternative version of the informed set, called the L^2 greedy informed set, which is approximated based on the exploited knowledge of the current solution path using the maximum admissible heuristic cost (Section III). Instead of using the cost of the current solution as an admissible heuristic for the informed set, the greedy informed set only considers the maximum heuristic cost along the current solution path. This results in smaller informed subsets and is shown to have better convergence properties than the informed set, typically in problems with complex initial solution paths.

This paper also studies the formal guarantees of the greedy informed set, analyzing how the use of heuristics affects optimality. If the true optimal solution path lies within the same homotopy class as the current solution path, the greedy informed set is guaranteed to include the states along the optimal path (Theorem 1). However, in certain planning problems where the optimal path and current solution path lie in different homotopy regions, the greedy informed set results in suboptimal solutions, failing to include the states along the optimal path (Theorem 2). This analysis shows that, depending on the nature of the problem domain, an appropriate balance between exploiting the greedy informed set and exploring with the larger informed set is essential to preserve the asymptotic optimality of informed sampling-based planners.

While direct informed sampling techniques prove effective compared to traditional space-filling approaches, their effectiveness only becomes apparent once an initial solution is found. Consequently, the benefits of focused sampling diminish in complex planning problems where finding an initial solution is challenging, especially in high-dimensional state spaces. Hence, finding a fast initial solution is crucial for sampling-based planning algorithms to leverage all the benefits of informed sets. This paper also presents an algorithm that uses bidirectional search to accelerate the process of finding initial solutions and leverages the greedy informed set to focus the search using exploited knowledge of the current solution.

To this end, this paper presents an almost-surely asymptotically optimal path planning algorithm that utilizes greedy heuristic techniques to address challenges in high-dimensional planning domains (Section IV). G-RRT* maintains two rapidly growing random geometric graphs (RGGs) to explore the problem state space and uses a greedy connection heuristic to guide the trees toward each other. This helps G-RRT* find faster initial solutions and often escape local minima with biased Voronoi regions.

G-RRT* also focuses the search on the L^2 greedy informed set once the initial solution is found, i.e., forward and reverse search trees meet each other. This allows G-RRT* to search efficiently on the smaller subset of the problem domain with exploited knowledge of the current solution path. Moreover, a greedy biasing ratio is introduced to balance uniform sampling from the problem domain (i.e., exploration with L^2 informed set) for optimal guarantees and path-biased sampling (i.e., exploitation with L^2 greedy informed set) for accelerating convergence. As a result, G-RRT* is probabilistically complete and almost-surely asymptotically optimal (Section V). We also analyze how the greedy biasing ratio affects the worst-case performance of sampling from the greedy informed set compared to sampling only from the informed set (Theorem 3).

The benefits of the greedy heuristic techniques are demonstrated on abstract planning problems, manipulation problems in simulations, and real-world trials with a self-reconfigurable robot, Panthera, across a range of dimensions (Section VI). The results from the experiments show that G-RRT* outperforms all the tested state-of-the-art asymptotically optimal planners, especially in high-dimensional problems. It often searches for faster initial solutions and finds better solutions with a faster convergence rate for problems seeking to minimize path length. We found that $\epsilon = 0.9$ is often sufficient to significantly improve the convergence rate of the algorithms in most planning problems (Section VI-C); however, this value can be adjusted according to specific needs.

Since the approximation and search in G-RRT* are based on a single sample per iteration, further research interest lies in extending the ideas of greedy informed sampling to batches of randomly generated samples, such as in Batch Informed Trees (BIT*) [44]. Additionally, we are currently investigating ways to define the promising regions of the problem domain, as we believe that exploiting these regions is crucial for improving the sampling efficiency and convergence rate of sampling-based motion planners in high-dimensional planning problems.

Information on the OMPL implementations of G-RRT* is publicly made available at https://github.com/mlsdpk/ompl.

Acknowledgements

The authors would like to thank Yunfan Lu for dedicating time to help with the proofs.

References

[1] S. M. LaValle, *Planning algorithms*. Cambridge university press, 2006.

[2] M. Elbanhawi and M. Simic, "Sampling-based robot motion planning: A review," *Ieee access*, vol. 2, pp. 56–77, 2014.

[3] J. H. Reif, "Complexity of the mover's problem and generalizations," in *20th Annual Symposium on Foundations of Computer Science (sfcs 1979)*. IEEE Computer Society, 1979, pp. 421–427.

[4] L. E. Kavraki, P. Svestka, J.-C. Latombe, and M. H. Overmars, "Probabilistic roadmaps for path planning in high-dimensional configuration spaces," *IEEE transactions on Robotics and Automation*, vol. 12, no. 4, pp. 566–580, 1996.

[5] S. M. LaValle and J. J. Kuffner Jr, "Randomized kinodynamic planning," *The international journal of robotics research*, vol. 20, no. 5, pp. 378–400, 2001.

[6] E. W. Dijkstra *et al.*, "A note on two problems in connexion with graphs," *Numerische mathematik*, vol. 1, no. 1, pp. 269–271, 1959.

[7] P. E. Hart, N. J. Nilsson, and B. Raphael, "A formal basis for the heuristic determination of minimum cost paths," *IEEE transactions on Systems Science and Cybernetics*, vol. 4, no. 2, pp. 100–107, 1968.

[8] S. Karaman and E. Frazzoli, "Sampling-based algorithms for optimal motion planning," *The international journal of robotics research*, vol. 30, no. 7, pp. 846–894, 2011.

[9] D. Ferguson and A. Stentz, "Anytime rrts," in *2006 IEEE/RSJ International Conference on Intelligent Robots and Systems*. IEEE, 2006, pp. 5369–5375.

[10] B. Akgun and M. Stilman, "Sampling heuristics for optimal motion planning in high dimensions," in *2011 IEEE/RSJ international conference on intelligent robots and systems*. IEEE, 2011, pp. 2640–2645.

[11] M. Otte and N. Correll, "C-forest: Parallel shortest path planning with superlinear speedup," *IEEE Transactions on Robotics*, vol. 29, no. 3, pp. 798–806, 2013.

[12] J. D. Gammell, S. S. Srinivasa, and T. D. Barfoot, "Informed rrt*: Optimal sampling-based path planning focused via direct sampling of an admissible ellipsoidal heuristic," in *2014 IEEE/RSJ International Conference on Intelligent Robots and Systems*. IEEE, 2014, pp. 2997–3004.

[13] J. J. Kuffner and S. M. LaValle, "Rrt-connect: An efficient approach to single-query path planning," in *Proceedings 2000 ICRA. Millennium Conference. IEEE International Conference on Robotics and Automation. Symposia Proceedings (Cat. No. 00CH37065)*, vol. 2. IEEE, 2000, pp. 995–1001.

[14] A. A. Hayat, R. Parween, M. R. Elara, K. Parsuraman, and P. S. Kandasamy, "Panthera: Design of a reconfigurable pavement sweeping robot," in *International Conference on Robotics and Automation (ICRA)*. IEEE, 2019, pp. 7346–7352.

[15] P. T. Kyaw, A. V. Le, P. Veerajagadheswar, M. R. Elara, T. T. Thu, N. H. K. Nhan, P. Van Duc, and M. B. Vu, "Energy-efficient path planning of reconfigurable robots in complex environments," *IEEE Transactions on Robotics*, vol. 38, no. 4, pp. 2481–2494, 2022.

[16] D. Hsu, L. E. Kavraki, J.-C. Latombe, R. Motwani, S. Sorkin *et al.*, "On finding narrow passages with probabilistic roadmap planners," in *Robotics: the algorithmic perspective: 1998 workshop on the algorithmic foundations of robotics*, 1998, pp. 141–154.

[17] O. Arslan and P. Tsiotras, "Use of relaxation methods in sampling-based algorithms for optimal motion planning," in *2013 IEEE International Conference on Robotics and Automation*. IEEE, 2013, pp. 2421–2428.

[18] S. Karaman, M. R. Walter, A. Perez, E. Frazzoli, and S. Teller, "Anytime motion planning using the rrt," in *2011 IEEE International Conference on Robotics and Automation*. IEEE, 2011, pp. 1478–1483.

[19] I.-B. Jeong, S.-J. Lee, and J.-H. Kim, "Quick-rrt*: Triangular inequality-based implementation of rrt* with improved initial solution and convergence rate," *Expert*

Systems with Applications, vol. 123, pp. 82–90, 2019.

[20] B. Liao, F. Wan, Y. Hua, R. Ma, S. Zhu, and X. Qing, "F-rrt*: An improved path planning algorithm with improved initial solution and convergence rate," *Expert Systems with Applications*, vol. 184, p. 115457, 2021.

[21] S. Klemm, J. Oberländer, A. Hermann, A. Roennau, T. Schamm, J. M. Zollner, and R. Dillmann, "Rrt-connect: Faster, asymptotically optimal motion planning," in *2015 IEEE international conference on robotics and biomimetics (ROBIO)*. IEEE, 2015, pp. 1670–1677.

[22] A. Dobson and K. E. Bekris, "Sparse roadmap spanners for asymptotically near-optimal motion planning," *The International Journal of Robotics Research*, vol. 33, no. 1, pp. 18–47, 2014.

[23] O. Salzman and D. Halperin, "Asymptotically near-optimal rrt for fast, high-quality motion planning," *IEEE Transactions on Robotics*, vol. 32, no. 3, pp. 473–483, 2016.

[24] J. Bialkowski, M. Otte, and E. Frazzoli, "Free-configuration biased sampling for motion planning," in *2013 IEEE/RSJ International Conference on Intelligent Robots and Systems*. IEEE, 2013, pp. 1272–1279.

[25] D. Kim, J. Lee, and S.-e. Yoon, "Cloud rrt: Sampling cloud based rrt," in *2014 IEEE International Conference on Robotics and Automation (ICRA)*. IEEE, 2014, pp. 2519–2526.

[26] A. H. Qureshi and Y. Ayaz, "Potential functions based sampling heuristic for optimal path planning," *Autonomous Robots*, vol. 40, pp. 1079–1093, 2016.

[27] Y. Li, W. Wei, Y. Gao, D. Wang, and Z. Fan, "Pq-rrt*: An improved path planning algorithm for mobile robots," *Expert systems with applications*, vol. 152, p. 113425, 2020.

[28] O. Khatib, "Real-time obstacle avoidance for manipulators and mobile robots," *The international journal of robotics research*, vol. 5, no. 1, pp. 90–98, 1986.

[29] F. Islam, J. Nasir, U. Malik, Y. Ayaz, and O. Hasan, "Rrt*-smart: Rapid convergence implementation of rrt* towards optimal solution," in *2012 IEEE international conference on mechatronics and automation*. IEEE, 2012, pp. 1651–1656.

[30] R. Alterovitz, S. Patil, and A. Derbakova, "Rapidly-exploring roadmaps: Weighing exploration vs. refinement in optimal motion planning," in *2011 IEEE International Conference on Robotics and Automation*. IEEE, 2011, pp. 3706–3712.

[31] J. D. Gammell, T. D. Barfoot, and S. S. Srinivasa, "Informed sampling for asymptotically optimal path planning," *IEEE Transactions on Robotics*, vol. 34, no. 4, pp. 966–984, 2018.

[32] M.-C. Kim and J.-B. Song, "Informed rrt* towards optimality by reducing size of hyperellipsoid," in *2015 IEEE International Conference on Advanced Intelligent Mechatronics (AIM)*. IEEE, 2015, pp. 244–248.

[33] H. Jiang, Q. Chen, Y. Zheng, and Z. Xu, "Informed rrt* with adjoining obstacle process for robot path planning," in *2020 IEEE 20th International Conference on Communication Technology (ICCT)*. IEEE, 2020, pp. 1471–1477.

[34] Z. Wang, Y. Li, H. Zhang, C. Liu, and Q. Chen, "Sampling-based optimal motion planning with smart exploration and exploitation," *IEEE/ASME Transactions on Mechatronics*, vol. 25, no. 5, pp. 2376–2386, 2020.

[35] J. Wang, C. X.-T. Li, W. Chi, and M. Q.-H. Meng, "Tropistic rrt: An efficient planning algorithm via adaptive restricted sampling space," in *2018 IEEE International Conference on Information and Automation (ICIA)*. IEEE, 2018, pp. 1639–1646.

[36] J. Wang, W. Chi, M. Shao, and M. Q.-H. Meng, "Finding a high-quality initial solution for the rrts algorithms in 2d environments," *Robotica*, vol. 37, no. 10, pp. 1677–1694, 2019.

[37] J. Wang, W. Chi, C. Li, C. Wang, and M. Q.-H. Meng, "Neural rrt*: Learning-based optimal path planning," *IEEE Transactions on Automation Science and Engineering*, vol. 17, no. 4, pp. 1748–1758, 2020.

[38] T. Zhang, J. Wang, and M. Q.-H. Meng, "Generative adversarial network based heuristics for sampling-based path planning," *IEEE/CAA Journal of Automatica Sinica*, vol. 9, no. 1, pp. 64–74, 2021.

[39] J. Wang, T. Li, B. Li, and M. Q.-H. Meng, "Gmr-rrt*: Sampling-based path planning using gaussian mixture regression," *IEEE Transactions on Intelligent Vehicles*, vol. 7, no. 3, pp. 690–700, 2022.

[40] A. Hatcher, *Algebraic Topology*. Cambridge University Press, 2002.

[41] T. H. Cormen, C. E. Leiserson, R. L. Rivest, and C. Stein, *Introduction to algorithms*. MIT press, 2022.

[42] R. Mashayekhi, M. Y. I. Idris, M. H. Anisi, I. Ahmedy, and I. Ali, "Informed rrt*-connect: An asymptotically optimal single-query path planning method," *IEEE Access*, vol. 8, pp. 19 842–19 852, 2020.

[43] I. A. Sucan, M. Moll, and L. E. Kavraki, "The open motion planning library," *IEEE Robotics & Automation Magazine*, vol. 19, no. 4, pp. 72–82, 2012.

[44] J. D. Gammell, T. D. Barfoot, and S. S. Srinivasa, "Batch informed trees (bit*): Informed asymptotically optimal anytime search," *The International Journal of Robotics Research*, vol. 39, no. 5, pp. 543–567, 2020.

[45] M. P. Strub and J. D. Gammell, "Adaptively informed trees (ait*): Fast asymptotically optimal path planning through adaptive heuristics," in *2020 IEEE International Conference on Robotics and Automation (ICRA)*. IEEE, 2020, pp. 3191–3198.

[46] ——, "Adaptively informed trees (ait*) and effort informed trees (eit*): Asymmetric bidirectional sampling-based path planning," *The International Journal of Robotics Research*, vol. 41, no. 4, pp. 390–417, 2022.

[47] R. Diankov, "Automated construction of robotic manipulation programs," Ph.D. dissertation, Carnegie Mellon University, USA, 2010.

[48] J. D. Gammell, M. P. Strub, and V. N. Hartmann, "Planner developer tools (pdt): Reproducible experiments and statistical analysis for developing and testing motion planners," in *Proceedings of the Workshop on Evaluating Motion Planning Performance (EMPP), IEEE/RSJ Inter-*

national Conference on Intelligent Robots and Systems (IROS), 2022.

[49] A. Yershova, L. Jaillet, T. Siméon, and S. M. LaValle, "Dynamic-domain rrts: Efficient exploration by controlling the sampling domain," in *Proceedings of the 2005 IEEE international conference on robotics and automation*. IEEE, 2005, pp. 3856–3861.

[50] J. Pan, S. Chitta, and D. Manocha, "Fcl: A general purpose library for collision and proximity queries," in *2012 IEEE International Conference on Robotics and Automation*. IEEE, 2012, pp. 3859–3866.

[51] M. Quigley, K. Conley, B. Gerkey, J. Faust, T. Foote, J. Leibs, R. Wheeler, and A. Y. Ng, "Ros: an open-source robot operating system," in *ICRA workshop on open source software*, vol. 3, no. 3.2. Kobe, Japan, 2009, p. 5.

[52] M. M. Rayguru, R. E. Mohan, R. Parween, L. Yi, A. V. Le, and S. Roy, "An output feedback based robust saturated controller design for pavement sweeping self-reconfigurable robot," *IEEE/ASME Transactions on Mechatronics*, vol. 26, no. 3, pp. 1236–1247, 2021.

[53] K. Koide, J. Miura, and E. Menegatti, "A portable 3d lidar-based system for long-term and wide-area people behavior measurement," *IEEE Trans. Hum. Mach. Syst*, 2018.

Phone Thiha Kyaw studied Mechatronics Engineering at Yangon Technological University, Yangon, Myanmar, from 2015 to 2021 and received a B.E. degree in Electronic Engineering from the University of Portsmouth, Portsmouth, England, in 2023. He also served as a visiting research fellow at the Robotics and Automation Research Laboratory (ROAR Lab) at the Singapore University of Technology and Design from 2019 to 2021. His research interests include task and motion planning of autonomous robotic systems, as well as the design of artificially intelligent agents using learning-based approaches.

Anh Vu Le received the B.S. degree in electronics and telecommunications from the Hanoi University of Technology, Vietnam, in 2007, and the Ph.D. degree in electronics and electrical from Dongguk University, South Korea, in 2015. He is currently with the Opto-electronics Research Group, Faculty of Electrical and Electronics Engineering, Ton Duc Thang University, Ho Chi Minh City, Vietnam. He is also a Postdoctoral Research Fellow with the ROAR Laboratory, Singapore University of Technology and Design. His current research interests include robotics vision, robot navigation, human detection, action recognition, feature matching, and 3D video processing.

Lim Yi received the B.Eng. and M.Eng. and PhD from the Engineering Product Development (EPD) Pillar, Singapore University of Technology and Design (SUTD), in 2017, 2020 and 2024, respectively. His current research interests include robotics, robotics control, robotics perception, robotics vision, and robotics navigation. He was awarded the Singapore University of Technology and Design President's Graduate Fellowship (Computing and Information Science Disciplines).

Prabakaran Veerajagadheswar received his Bachelor degree in Electronics and Instrumentation Engineering from Sathyabama University, India in 2013, and Ph.D. degree in Advanced engineering form Tokyo Denki University in 2019. Currently, he is working as a Research Fellow in ROARS LAB at Singapore University of Technology and Design. He won SG Mark Design Award in 2017 for the designing of h-Tetro, a self-reconfigurable cleaning robot. His research interest includes the development of complete coverage path planning, SLAM framework and embedded control for reconfigurable, and climbing robots. He is also a visiting instructor for a design course of International Design Institute at Zhejiang University, China.

Minh Bui Vu was born on March 02, 1991, in Dong Nai, Vietnam. He graduated in Electrical and Electronic Engineering in 2015 from Nguyen Tat Thanh University, Ho Chi Minh City, Vietnam. End of 2014, he joined the Faculty of Engineering and Technology of Nguyen Tat Thanh University as Laboratory-Practice management, until in 2017 he was a lecturer. In 2019, he received a Master's degree in Electrical Engineering from Ho Chi Minh City University of Technology and Education, Ho Chi Minh City, Vietnam. His major research interests are Wireless Networks, Robot, Artificial Neural Networks, Power Electronics.

Mohan Rajesh Elara is currently an Assistant Professor with the Engineering Product Development Pillar at Singapore University of Technology and Design (SUTD). He received his Ph.D. and M.Sc degrees from the Nanyang Technological University in 2012 and 2005. He obtained his B.E degree from the Bharathiar University, India in 2003. His research interests are in robotics with an emphasis on self-reconfigurable platforms as well as research problems related to robot ergonomics and autonomous systems. He has published more than 80 papers in leading journals, books, and conferences. He is the recipient of SG Mark Design Award in 2016 and 2017, ASEE Best of Design in Engineering Award in 2012, and Tan Kah Kee Young Inventors' Award in 2010. He is also a visiting faculty member of International Design Institute at Zhejiang University, China.